Nuclear Physics

EUROPEAN UNION

GOVERNMENT OF ROMANI

N-HH

Structural Instruments 2007-2013

Project co-financed by the European Regional Development Fund

Sectoral Operational Programme
„Increase of Economic Competitiveness"
"Investments for Your Future"

Nuclear reactions induced by laser accelerated beams

Florin Negoita for ELI-NP team

Laser Acceleration in short

- high-power (100 TW – 10 PW), short-pulse (few fs) lasers
- focused intensity on target: 10^{20} – 10^{24} W/cm^2

Electron acceleration (gas jet)

LWFA

(laser wake-field acceleration)

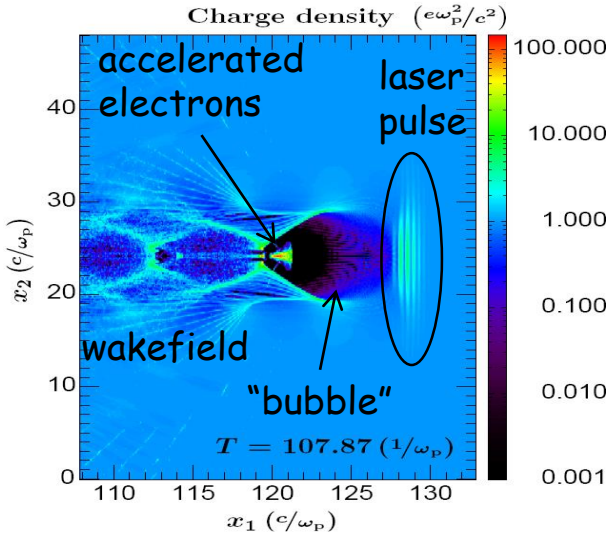

- field ~ TV/m
- E_e ~ GeV
- $E_{ion} \leq 150$ MeV/u
- charge ~ 10's of pC
- $\Delta E/E$ ~ 1-2% (e^-)
  ~ 10-20% (ion)
- $\varepsilon \sim 10^{-5}$ mm mrad

Ion acceleration (thin foil)

TNSA & RPA

(radiation-pressure acceleration)

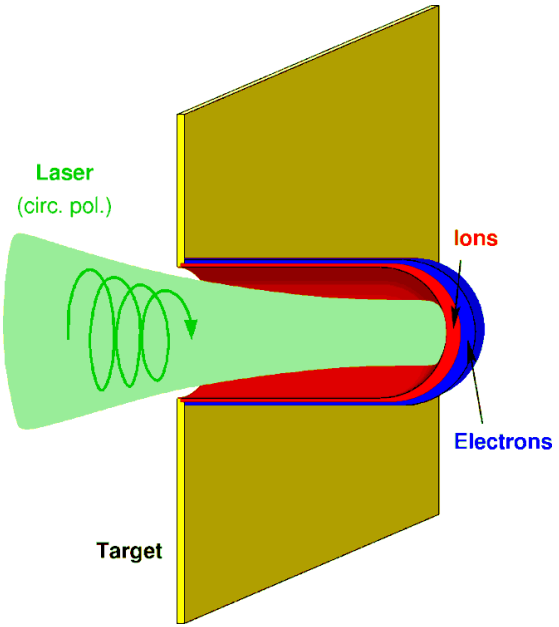

E. Esarey et al., Rev. Mod. Phys. 81 (2009) 1229

Main application: X-ray source, XFEL for material and life sciences

A. Henig et al., PRL 103 (2009) 245003.

Main application: hadrontherapy

Main focus at ELI-Beamlines (Czech Republic)

Astrophysical r process: waiting point N=126

- r process:
  - path for heavy nuclei far in ‚terra incognita'
  - astrophysical site(s) still unknown:

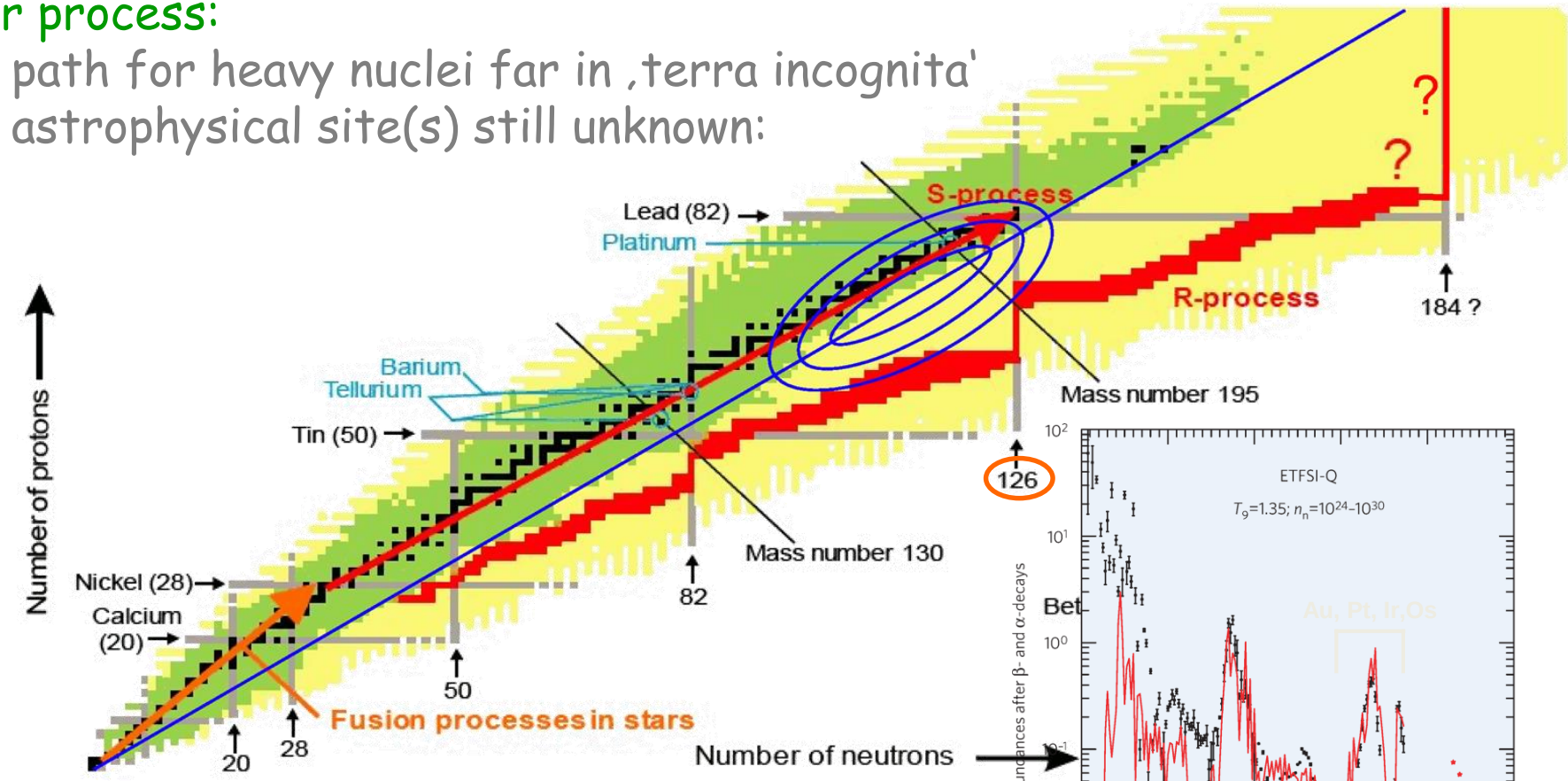

- waiting point N=126: bottleneck for nucleosynthesis of actinides
- last region of r process 'close' to stability

Fission – Fusion Mechanism

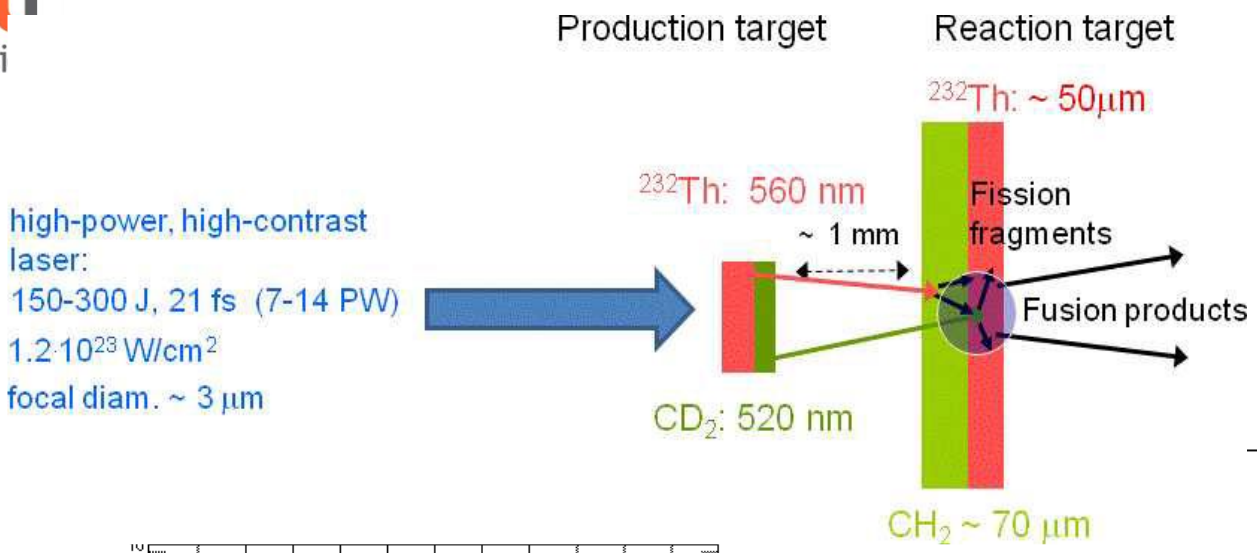

Mass distribution in Th fission

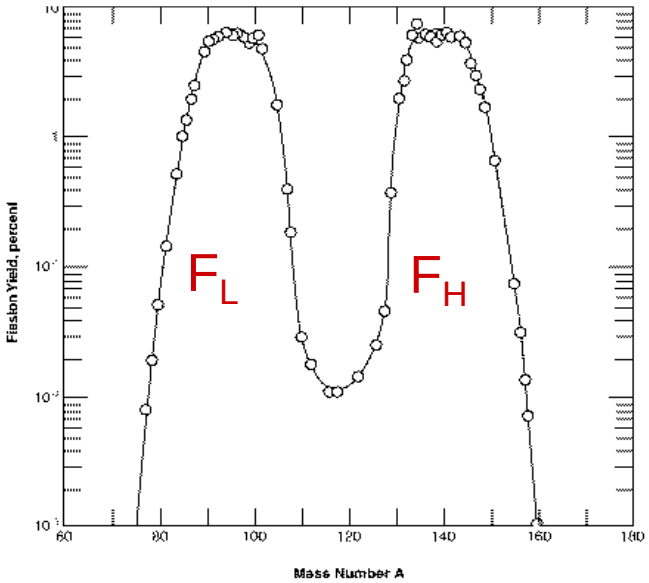

^{232}Th:

$\langle A_L \rangle \sim 91$

$\Delta A_L \sim 14$ amu (FWHM)

$\Delta AL \sim 22$ amu (10%)

$\langle Z_L \rangle \sim 37.5$ (Rb,Sr)

	Normal stopping	Reduced stopping
Production target:		
^{232}Th	560 nm	560 nm
CD_2	520 nm	520 nm
Accelerated Th ions	1.2×10^{11}	1.2×10^{11}
Accelerated deuterons	2.8×10^{11}	2.8×10^{11}
Accelerated C ions	1.4×10^{11}	1.4×10^{11}
Reaction target:		
CH_2	70 μm	–
^{232}Th	50 μm	5 mm
Beam-like light fragments	3.7×10^{8}	1.2×10^{11}
Target-like fission probability	2.3×10^{-5}	2.3×10^{-3}
Target-like light fragments	3.2×10^{6}	1.2×10^{11}
Fusion probability	1.8×10^{-4}	1.8×10^{-4}
Fusion products	1.5	4×10^{4}

In-flight Separator for ELI-NP

concept proposed by H. Geissel (GSI/U Giessen)
for separation of nuclei of interest from all other
accelerated particles and reaction products

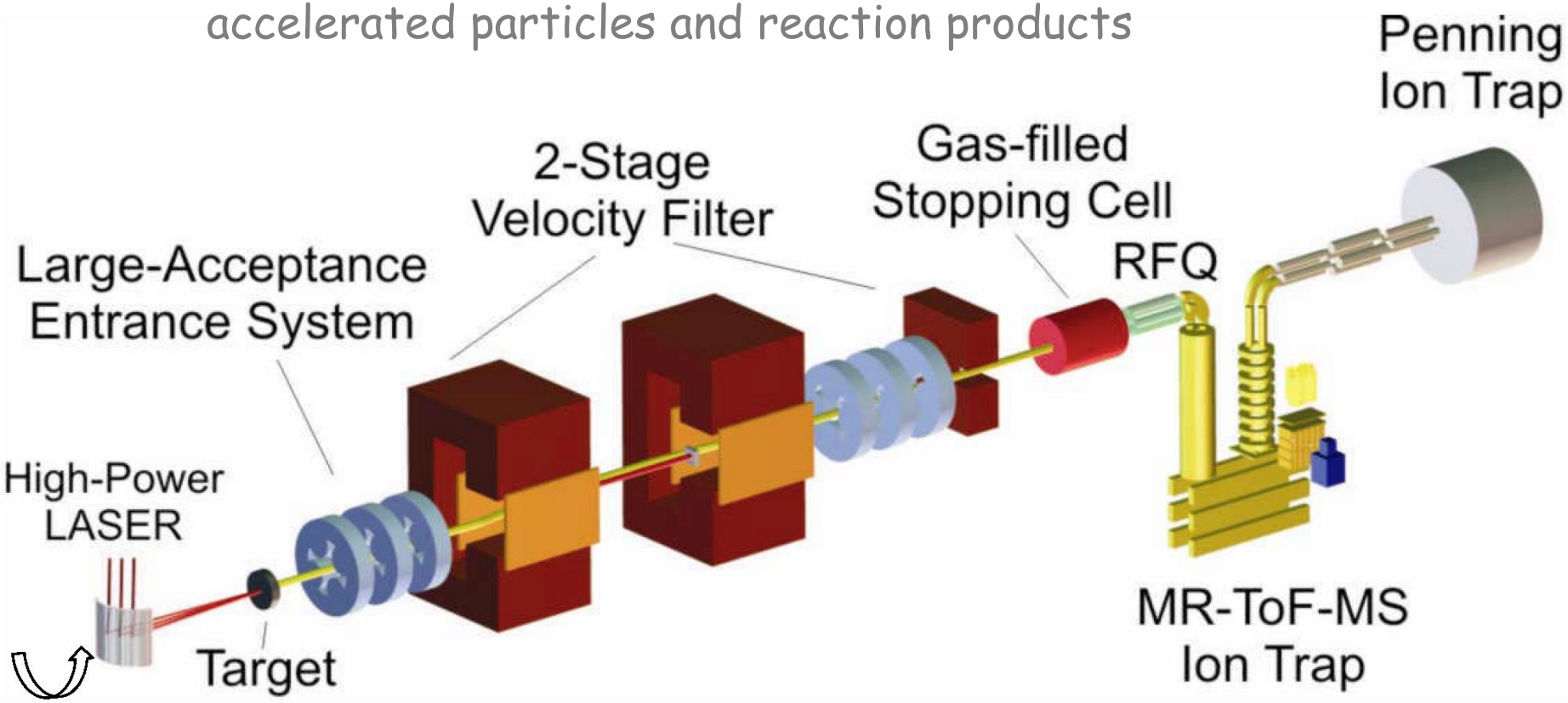

Measuring basic properties of N~126 nuclei: masses
lifetimes
decay modes

Fast Transport System to the Decay Station for high resolution gamma spectroscopy

Ph. Dessagne et al., DESIR @ SPIRAL2 TDR

M. Eibach et al., NIM A 613 (2010) 226

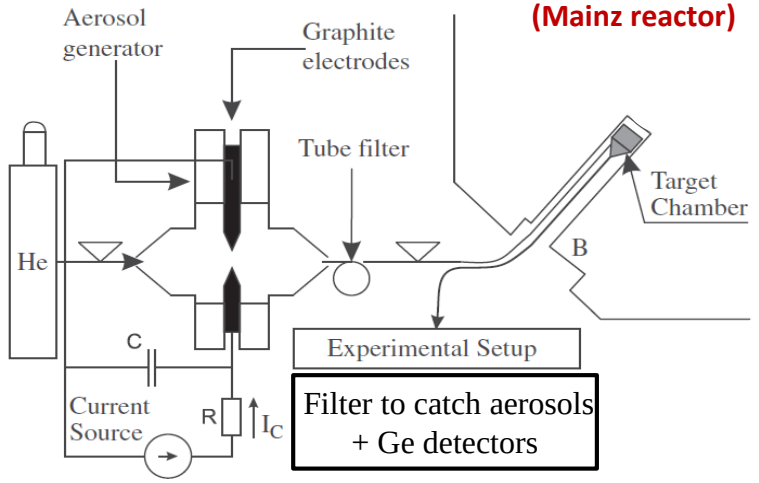

Carbon clusters aerosol (Mainz reactor)

Other aerosol possible: NaI (600 °C) or $PbCl_2$ (430 °C)

	Fast Tape Station Transport System	Gas-jet Transport System
Pro's	• Constant (measurable) transport efficiency • No servicing required over large operating time • Well defined transport time	• Suitable for both linear and non-linear long transport paths (a)
Limitations	• Tested speeds of up to 5 m/s (pre-acceleration could improve transport times)	• Variable transport efficiency 45-65% over several running hours • Wide distribution of the transport time typically in the range of 0.4-1 s for a 7 m path
Con's	• Mechanically challenging for transport over large distances and/or non-linear paths	• Need for regular maintenance each 1-2 UT's • Changer the filter ?

Mixed solution: aerosol + tape system at ELI-NP (S.-W. Xu et al., PRC 71 (2005) 054318)

Nuclear Reactions in Plasma

Study of screening factor in nuclear reactions of astrophysical interest

Proposal of S. Tudisco et al. – INFN-LNS (Italy)

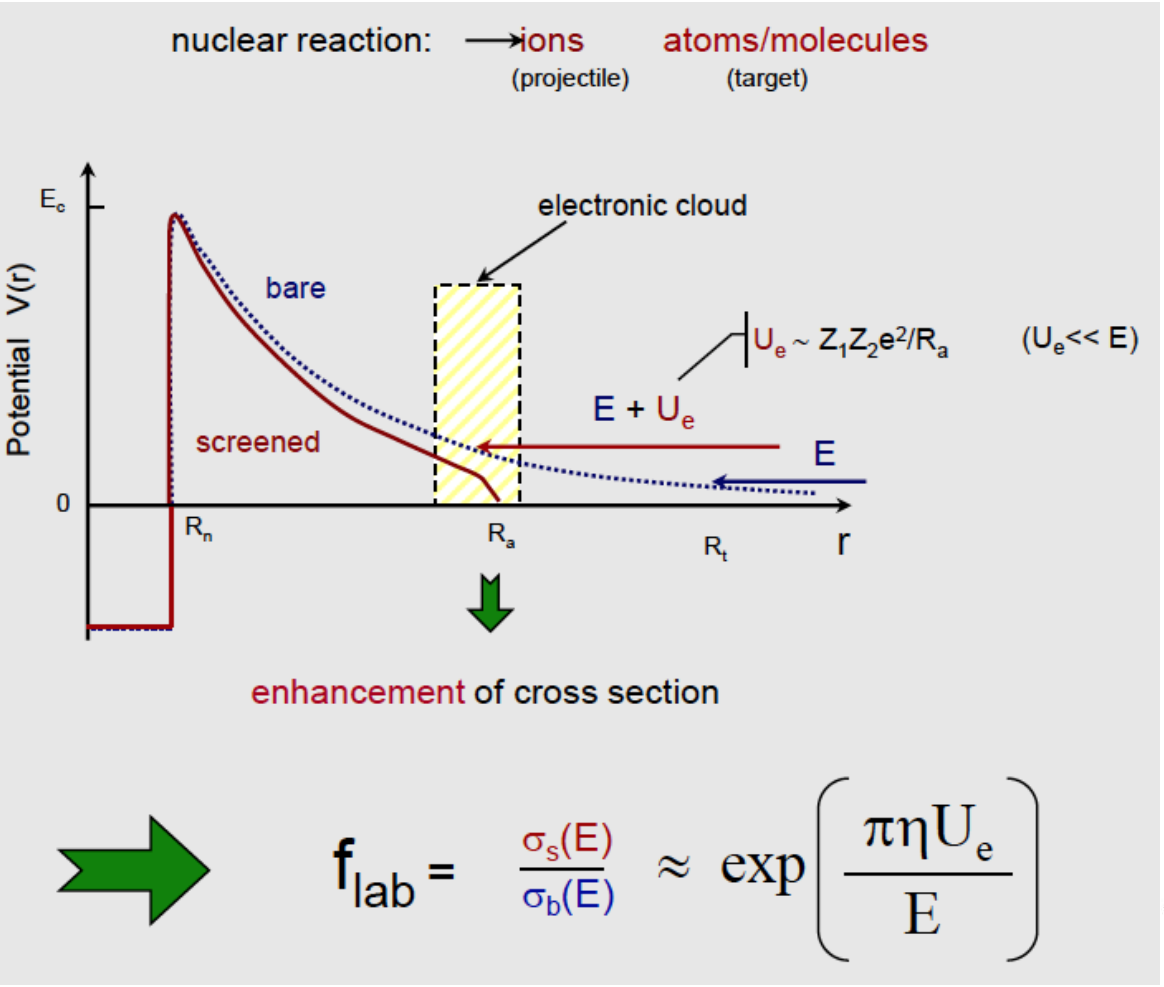

$\sigma(E) = 1/E \; \exp(-2\pi\eta) \; S(E)$

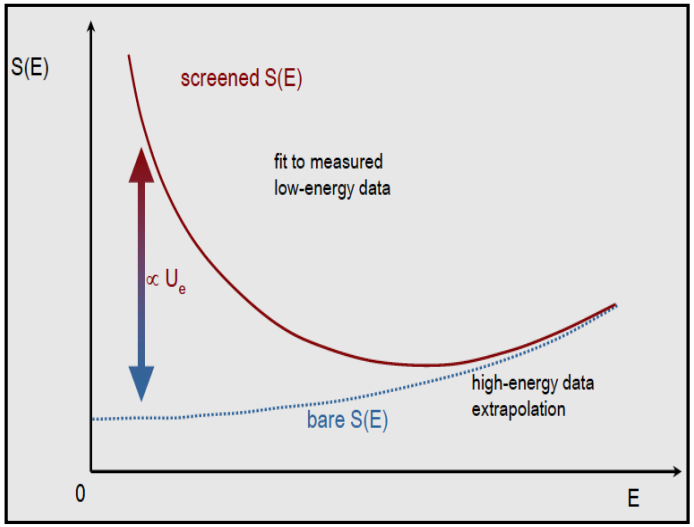

Extrapolation toward low energy is complicated by screening

Salpeter formula:

$$f = \exp\left(\frac{Z_1 Z_2 e^2}{R_D kT}\right) = \exp\left(0.188\, Z_1 Z_2 \zeta \rho^{1/2} T_6^{-3/2}\right)$$

Study of screening factor – The method and cases

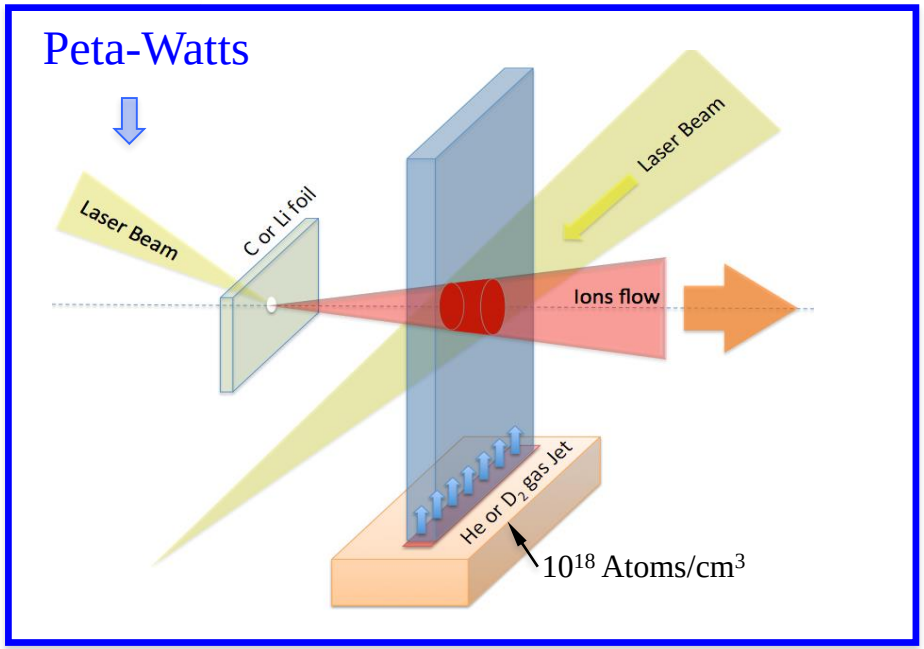

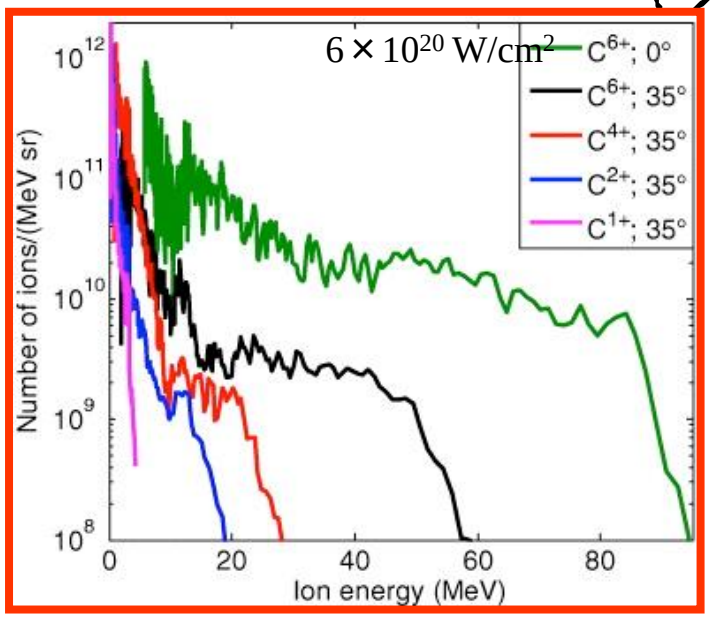

D.C. Carrol et al., New J. of Phys. 12 (2010) 045020

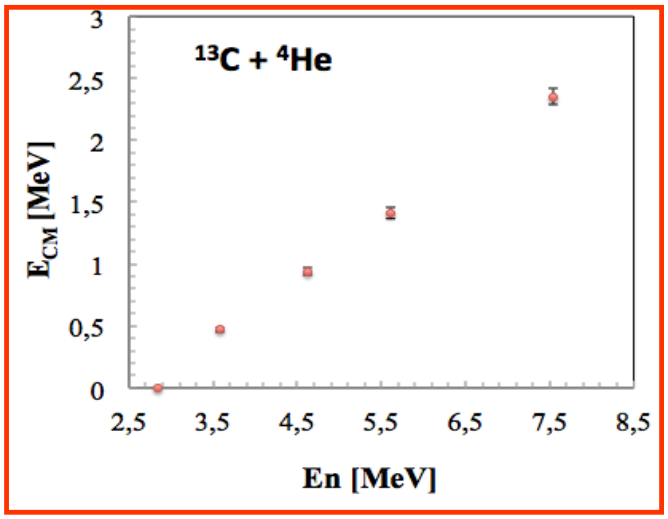

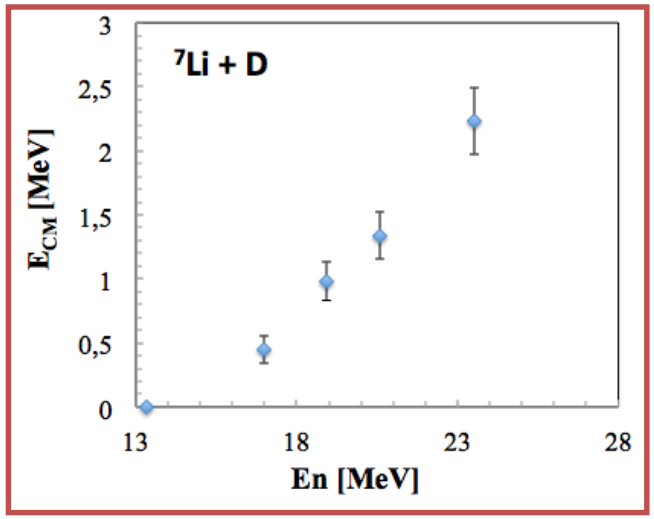

The method requires measuring high energy neutrons.

Nuclear (de-)excitations in plasma

Proposal of F.Hannachi et al. (CENBG)

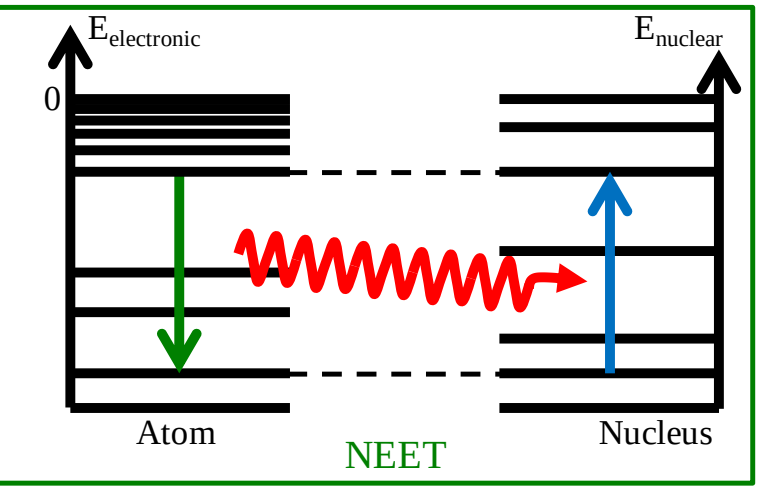

NEET observed in cold targets. Never observed in plasma.

NEEC was never observed

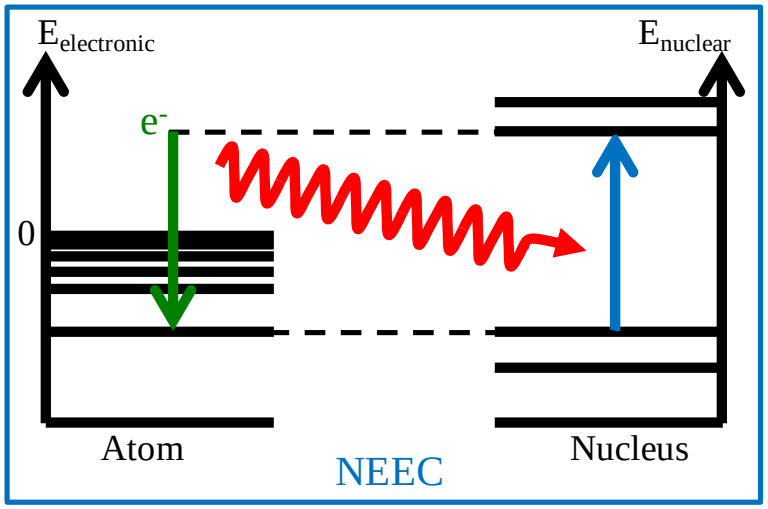

Significant changes in lifetimes are predicted in plasma conditions:

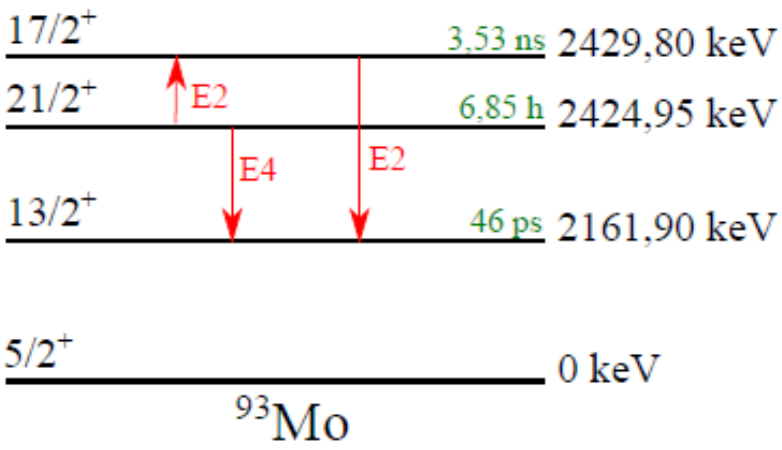

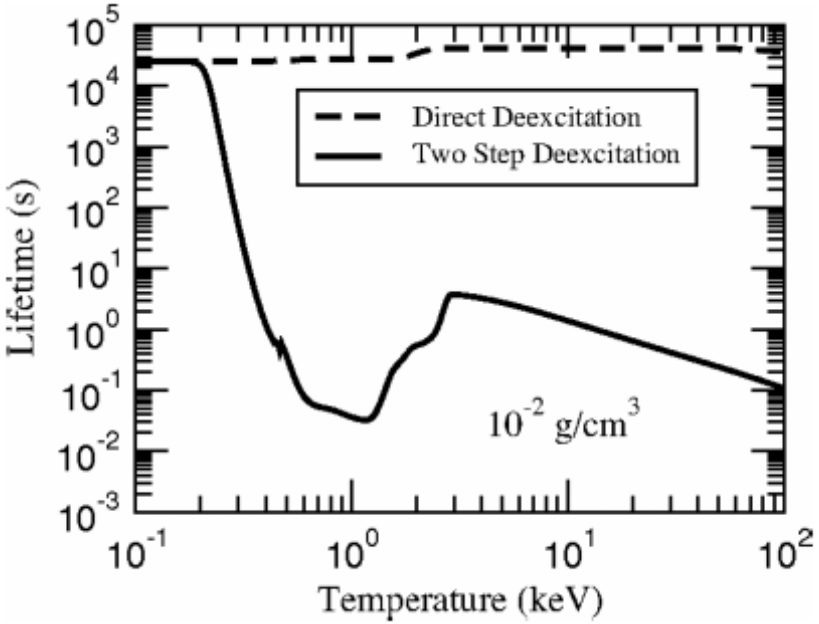

Nuclear excitations in plasma: ^{84m}Rb case

- Calculation of nuclear excitation rates by NEET and NEEC: need of a description of the atomic states in plasmas

$$\lambda_{NEET,NEEC} = \boxed{\text{Atom}} + \boxed{\text{Plasma}} + \boxed{\text{Nucleus}}$$ Very difficult !

  - ISOMEX based on a Relativistic Average Atom Model under Local Thermodynamic Equilibrium (LTE) hypothesis: all the ions in plasmas are described by one average ion
  - New model developed at CENBG

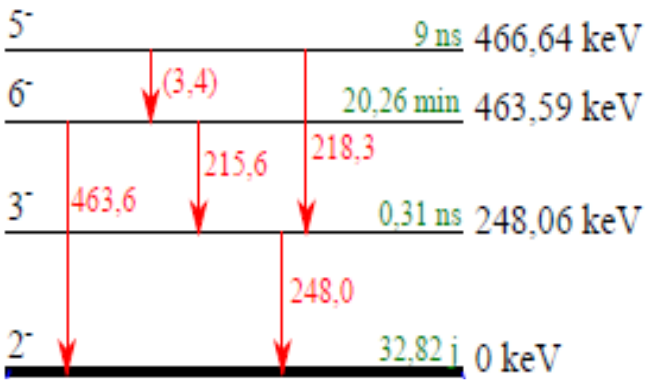

Gosselin et al., Private Communication

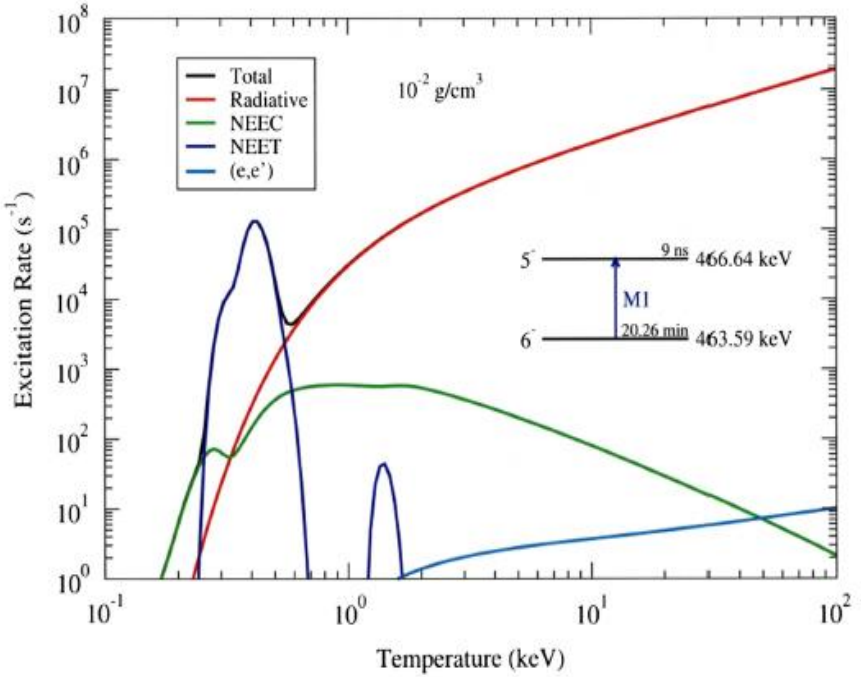

Nuclear excitations in plasma: proposed experiment

Experiment proposed:

- one 10 PW beam accelerated ions interacting with primary target
- ion produce isomeric states in a secondary solid target
- one uncompressed beam (~ 250 J / 1 ns) focussed to 10^{15} W/cm^2 used to produce plasma (focusing at ~ 100 μm)
- measure delayed gamma from isomer de-excitation

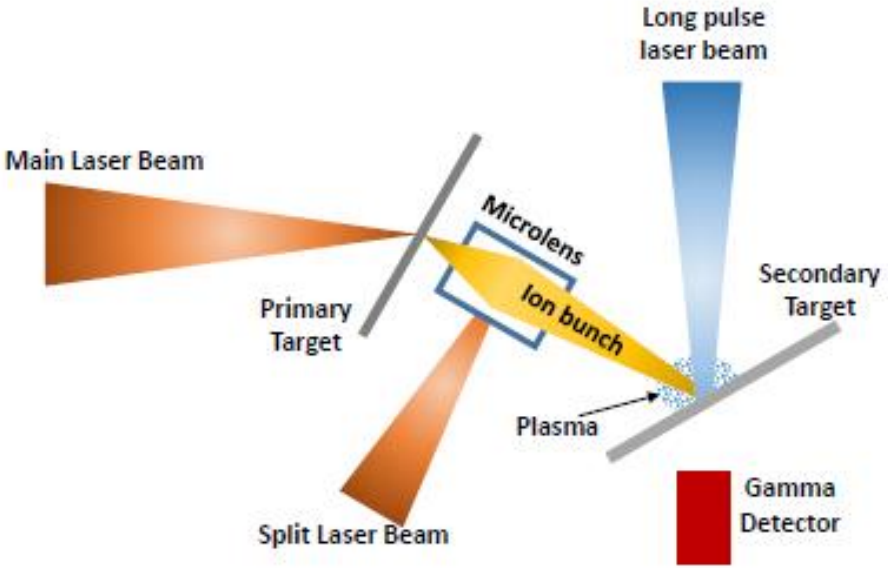

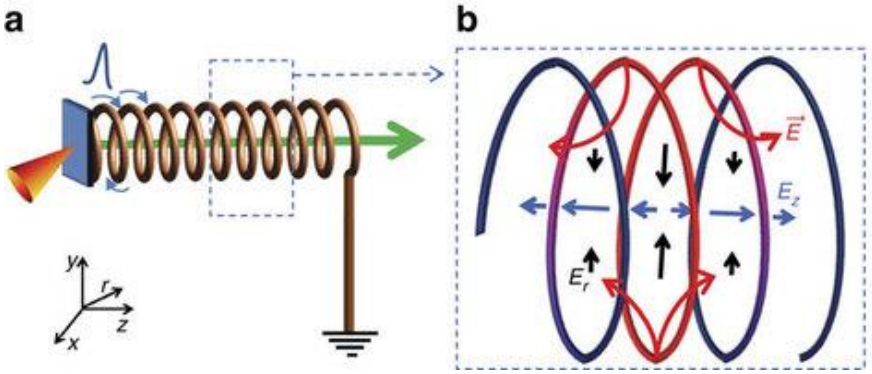

S. Kar et al.,Nature Comm. 7 (2016)

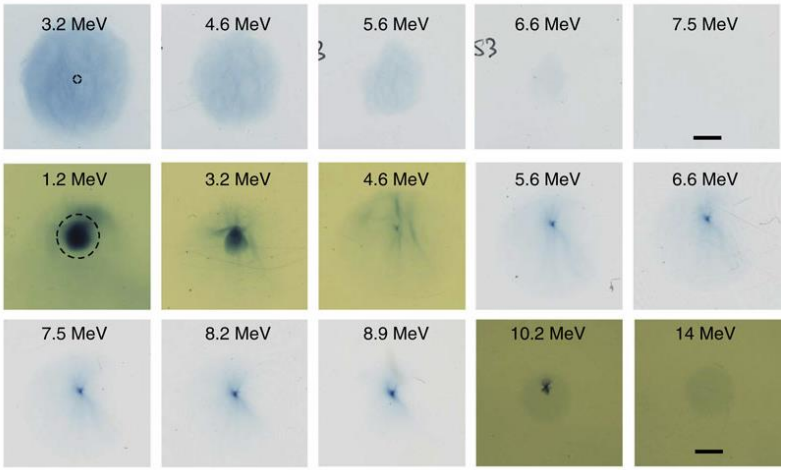

Nuclear excitation in plasma: ^{26}Al case
Proposal of K. Spohr et al.(SUPA)

- The 1809 keV gamma emission associated with the decay of ^{26}Al ($T_{1/2}=7.2\times10^5$ y) ground state was first observed gamma ray proving on-going nucleosynthesis.
- Still highly relevant observable in astrophysics.
- Lifetime changes in high temperature plasma predicted up to a factor of 10^9 by A.Coc, M.G.Porquet F. Nowacki [PRC61(199)015801]

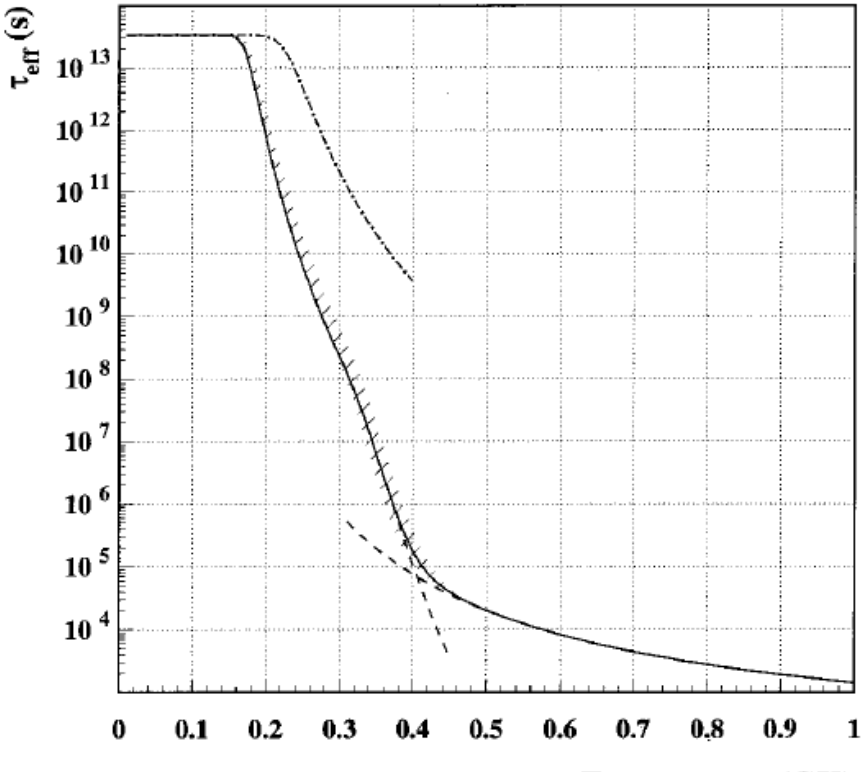

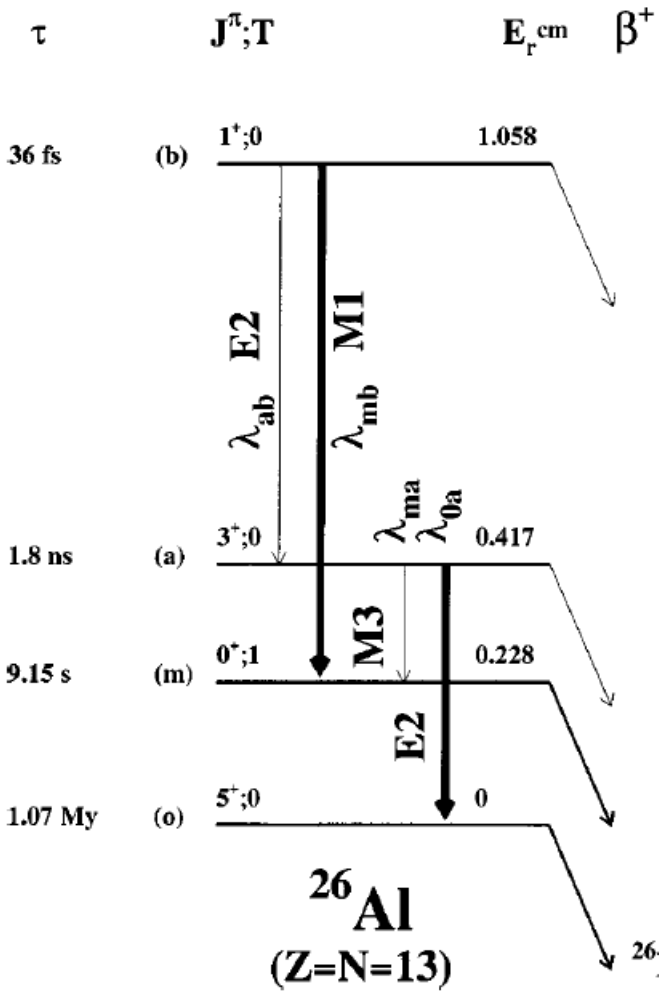

Neutron production

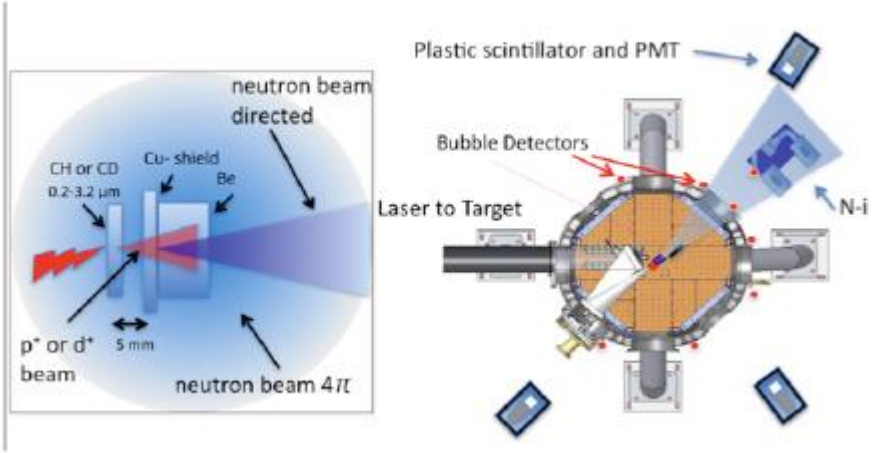

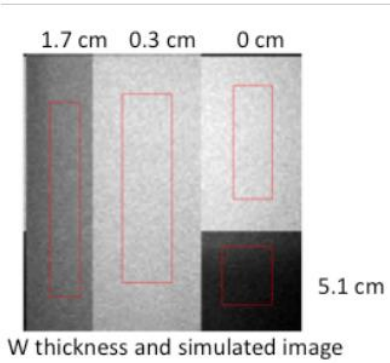

W thickness and simulated image

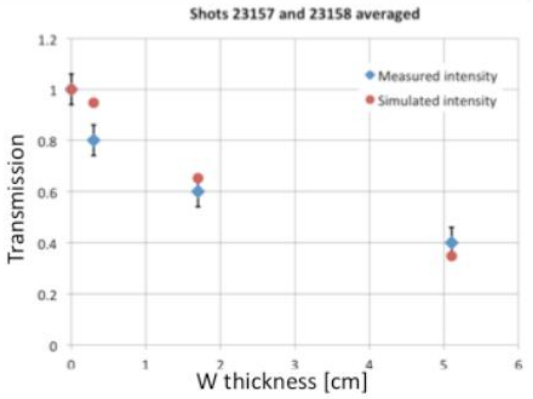

Trident facility (Los Alamos)

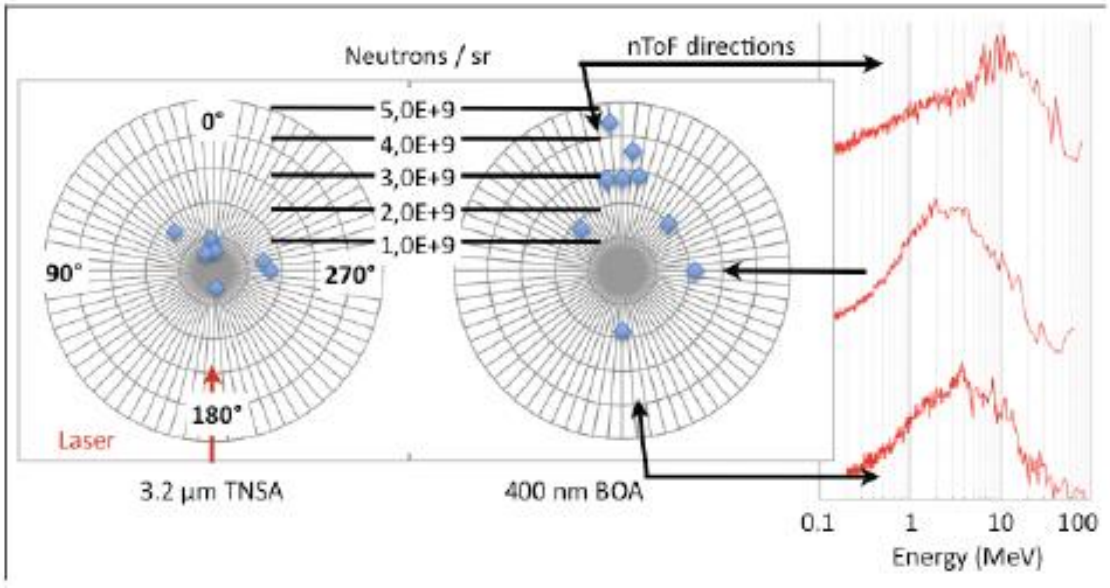

M. Roth et al.
PRL **110**, 044802 (2013)

More than 10^{10} n/pulse
Expected at ELI-NP

Laser-g conversion in high density low-Z targets

Laser-γ conversion efficiency in solid targets (*McKenna et al TDR2*)

5-10PW, F/3

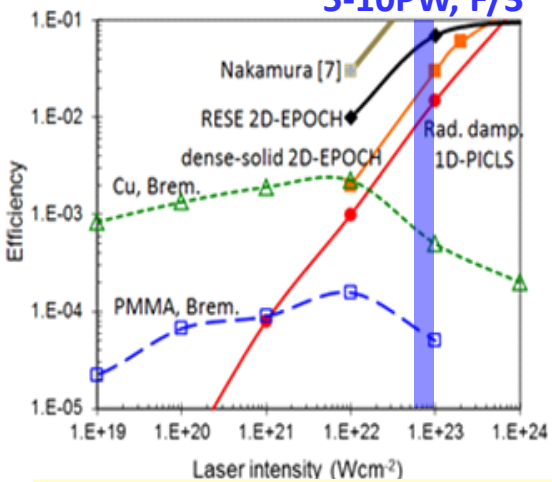

γ-ray spectrum and angular distribution for dense H jet at $I=10^{23}$ W/cm^2, $N_e = 4xN_{crit}$ *(Ribevre et al Phys Rev E 2016)*

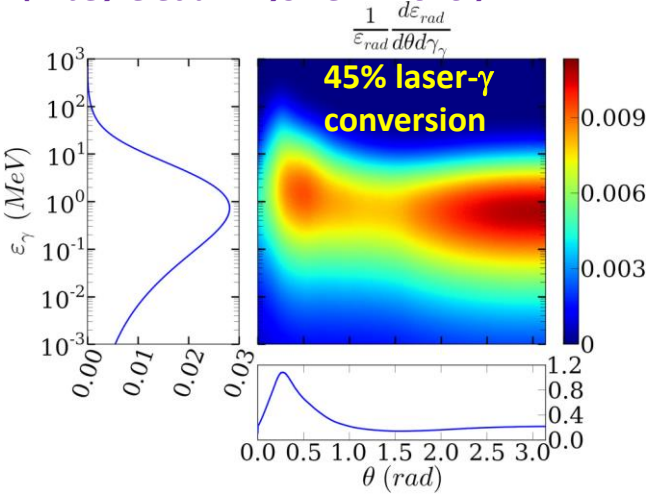

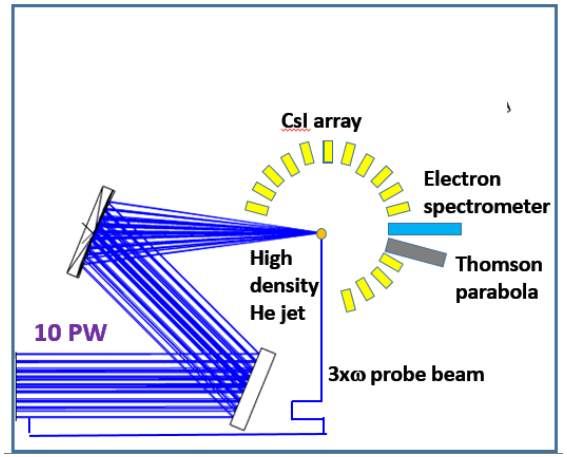

- Orders of magnitude increase above bremsstrahlung in all PIC-QED models
- 90% laser absorption and 45% laser-γ conversion in near-critical H jet
- Few MeV mean γ energy, angular distribution broadening rapidly with intensity
- First experiment: Scale γ production in dense He or H jet as a function of focal intensity in the range 10^{21} -10^{23} W/cm^2
- Absolute conversion efficiency can also be measured, but not critical

Neutron Production in Photonuclear Reactions

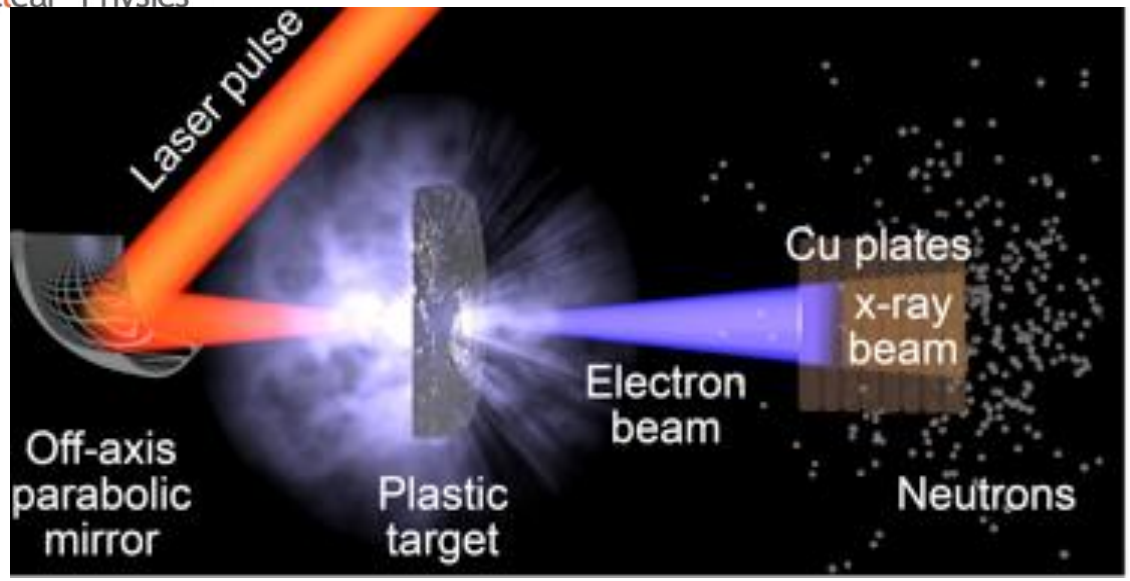

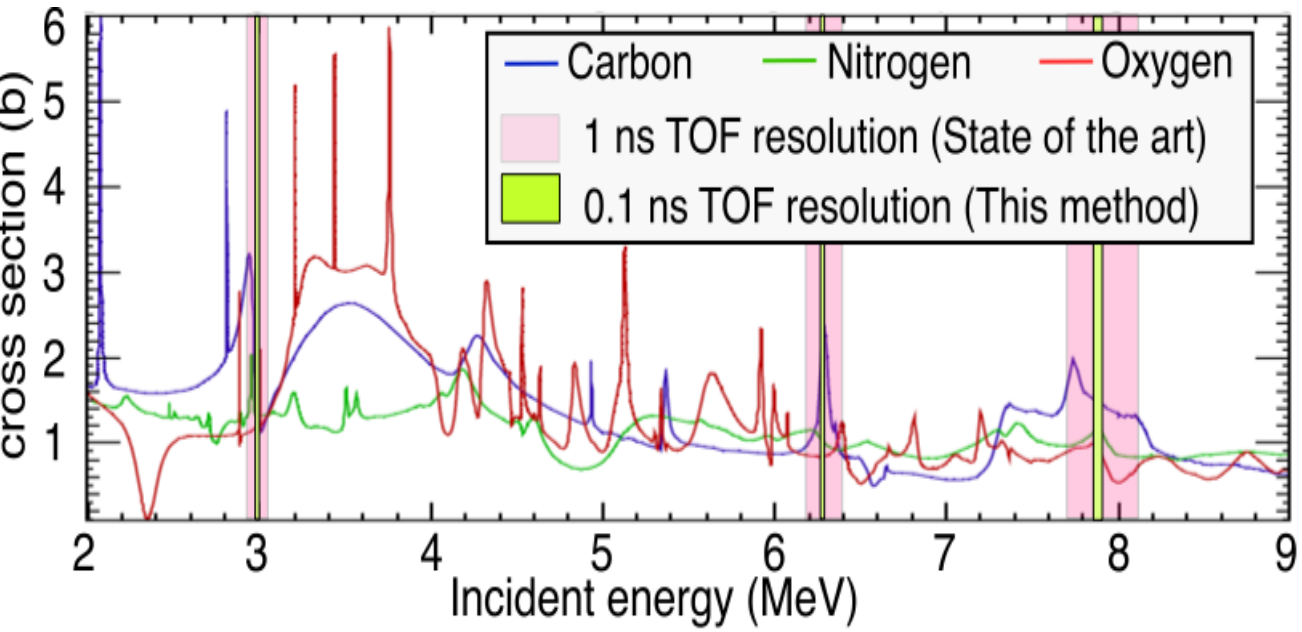

Proposal of I. Pomerantz, Univ. Tel-Aviv

more than 10^9 n/pulse with **50 ps pulse duration** expected at ELI-NP

Active and passive diagnostics

A full range of active and passive detector employed by high-power laser experiments at other facilities and adapted to ELI-NP:

- proton or ion spectrometers
  - passive: Thomson parabola + IPs, RCF stacks
  - active: Thomson parabola + scintillator (or MCP+screen) + CCD
- gamma detectors:
  - prompt spectrum
  - short lived states with in-situ LaBr3 scintillators
  - off-line (activation) detectors
- neutron detectors: scintillators, bubble detectors
- plasma diagnostics and electromagnetic fields (Optical, THz, XUV) including fast probe beams

Several detectors specific to ELI-NP

POSTPONED

- Decay station with Ge detectors
- Recoil separator
- Stopping gas cell and RFQ and MR-TOF or Penning traps

X-ray Backlighter for High Density Plasma Characterisation

Proposal of D. Stutman et al.

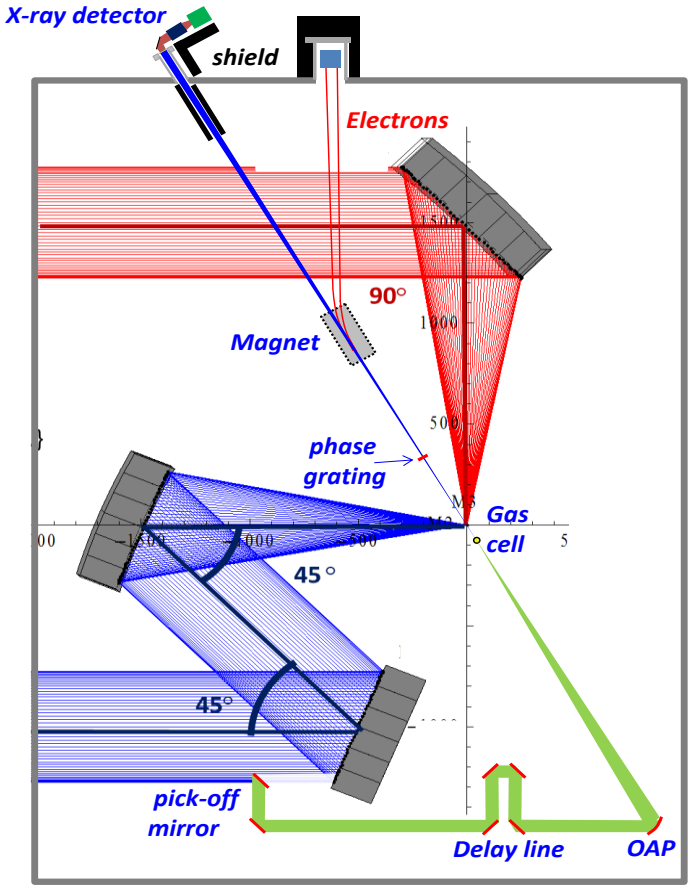

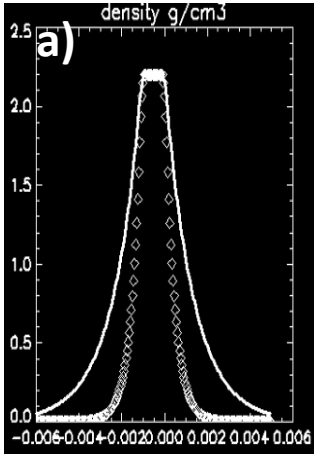

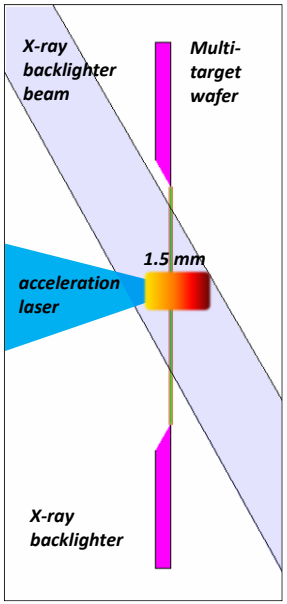

Zoom around target position

Two target density profiles assumed in the simulation, and calculated X-ray intensity profiles.

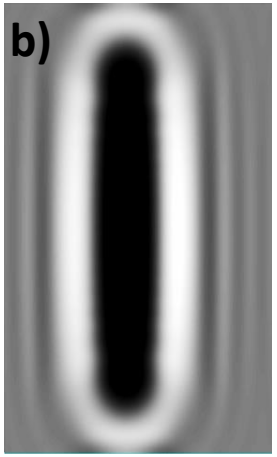

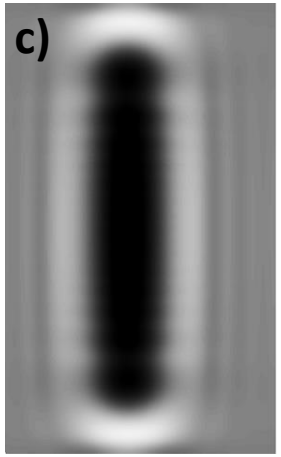

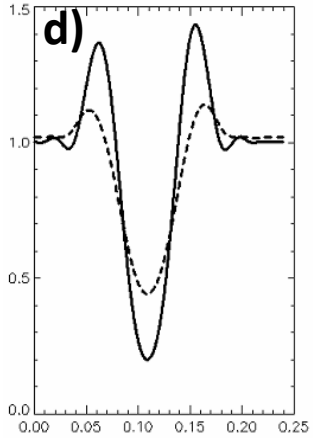

Using betatron emission occuring during LWFA electron acceleration in gas as probe beam for high density plasma.

Gamma detectors: Attenuators & IP stack

proof of principle setup:

Jeon *et al.*, Rev. Sci. Instrum. 86 (2015) 123116

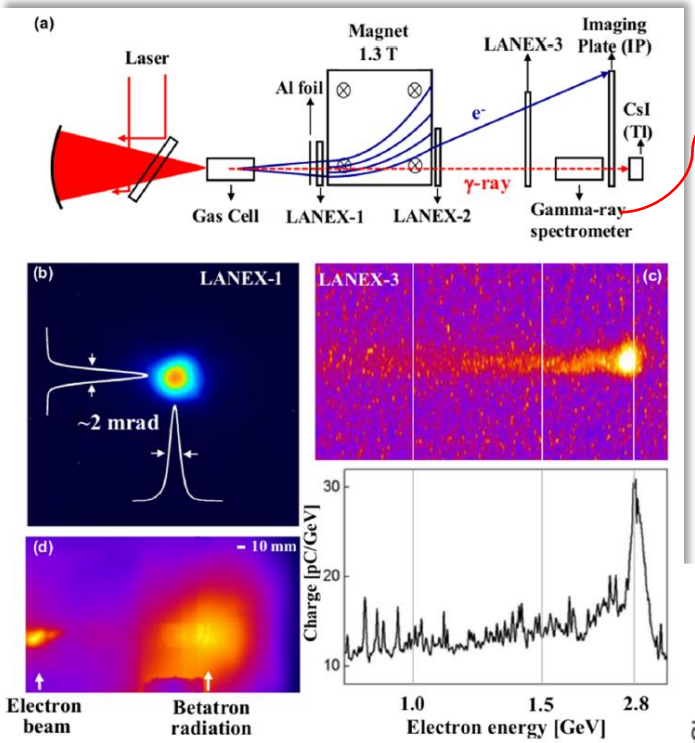

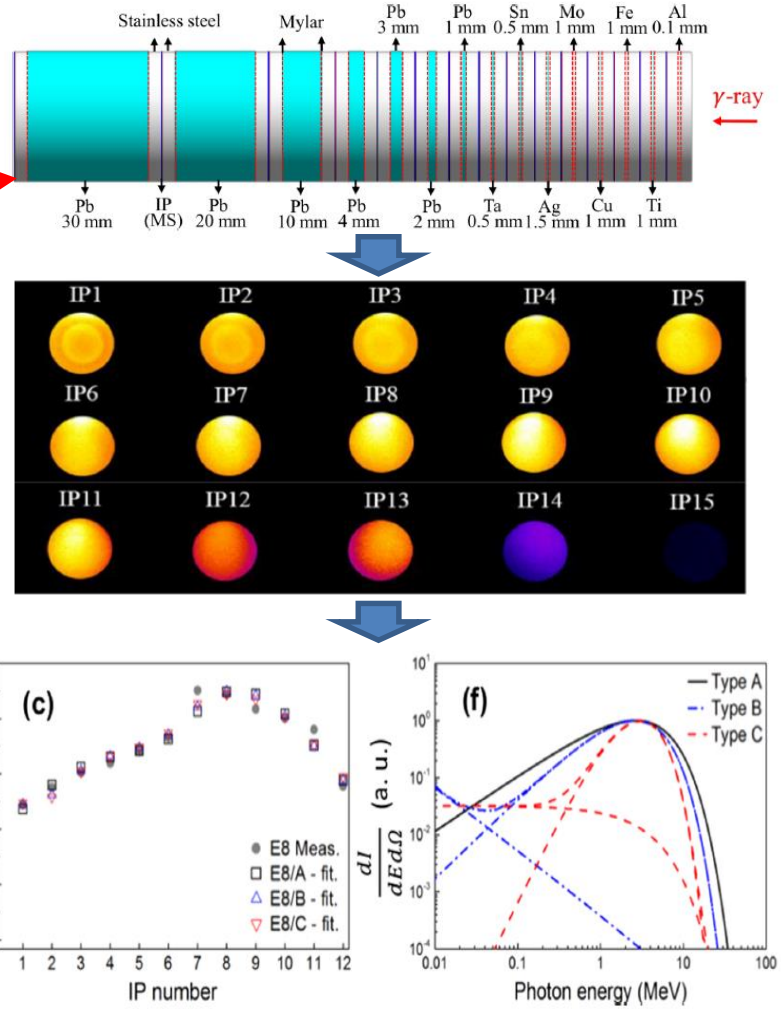

Gamma detectors: Array of CsI scintillators

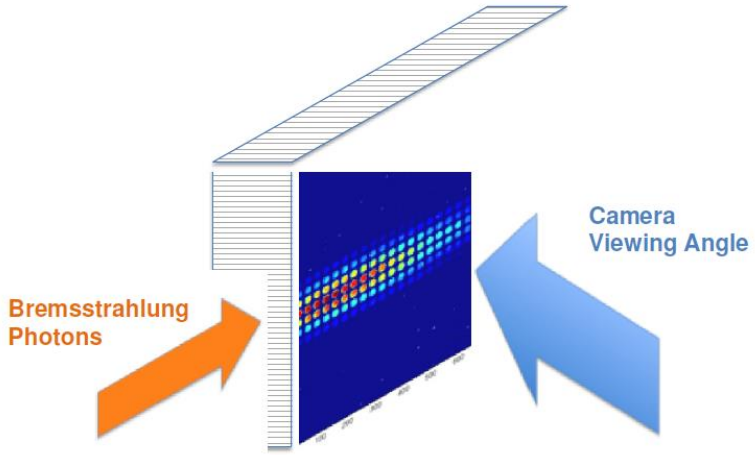

Fig2: Geometry of the CsI array detector and CCD camera relative to bremsstrahlung source

30x30 array of CsI bars (5 x 5 x 30

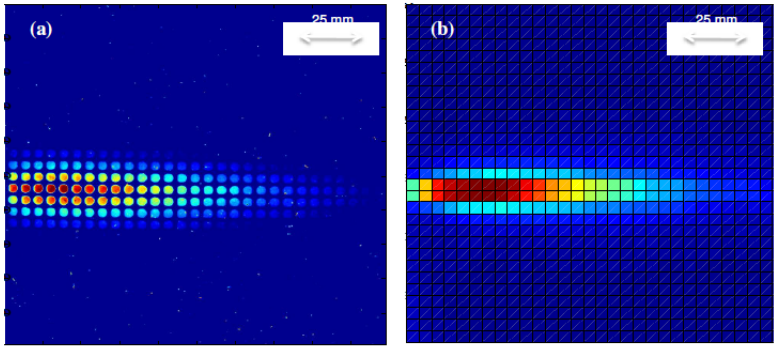

Fig4: (a) Image of CsI detector recorded by the CCD camera from the experiment; (b) Image of CsI detector generated by Geant4

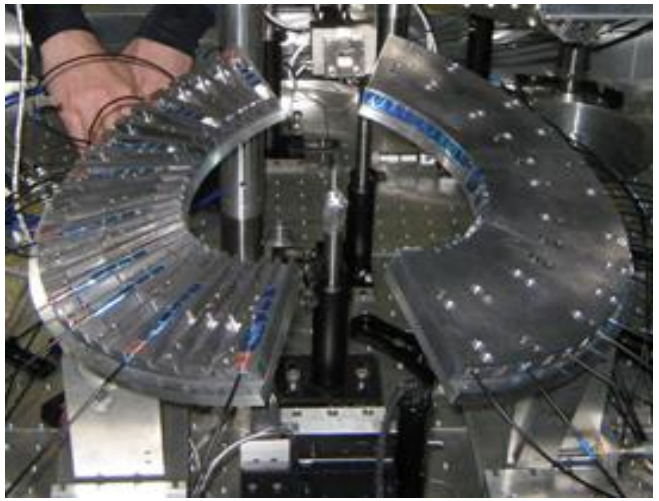

CsI array for angle resolved calorimetry

"Left" solution seems good for low divergence. The "right" solution is good for large angular distribution. We may go for a "mixed" solution, Such as few stack of 4-5 detectors, placed at just few angles.

0 deg. Compton scattering spectrometry (b)

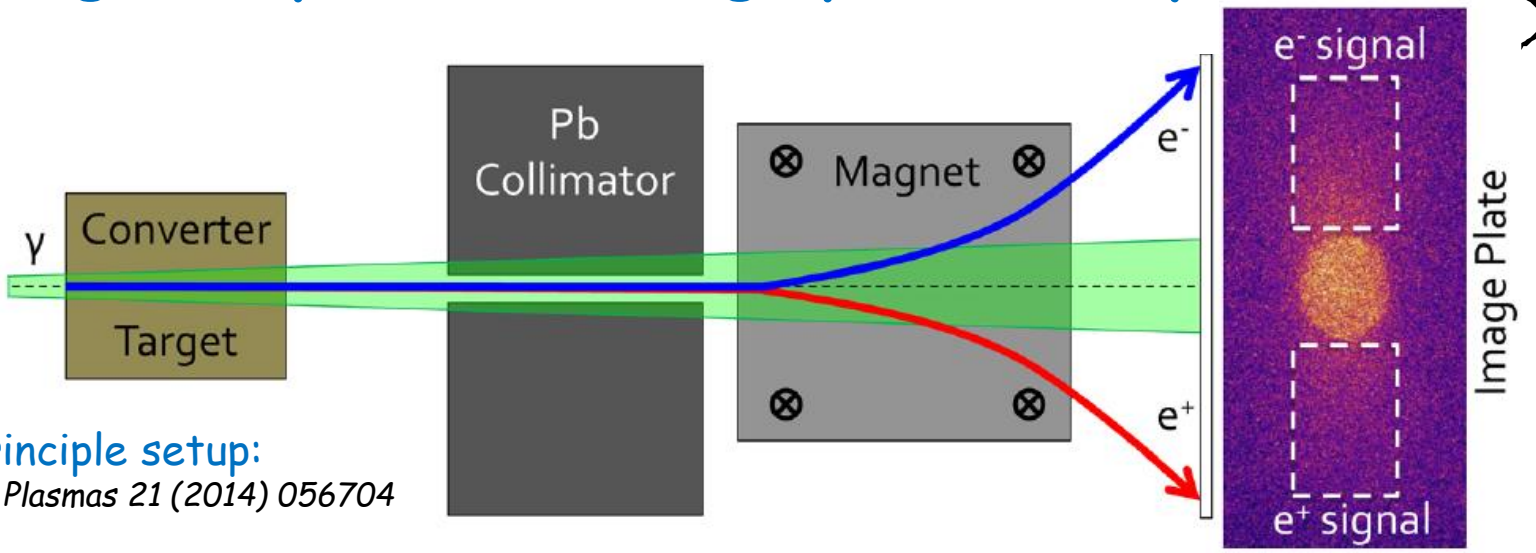

proof of principle setup:

Schumaker et al., Phys. Plasmas 21 (2014) 056704

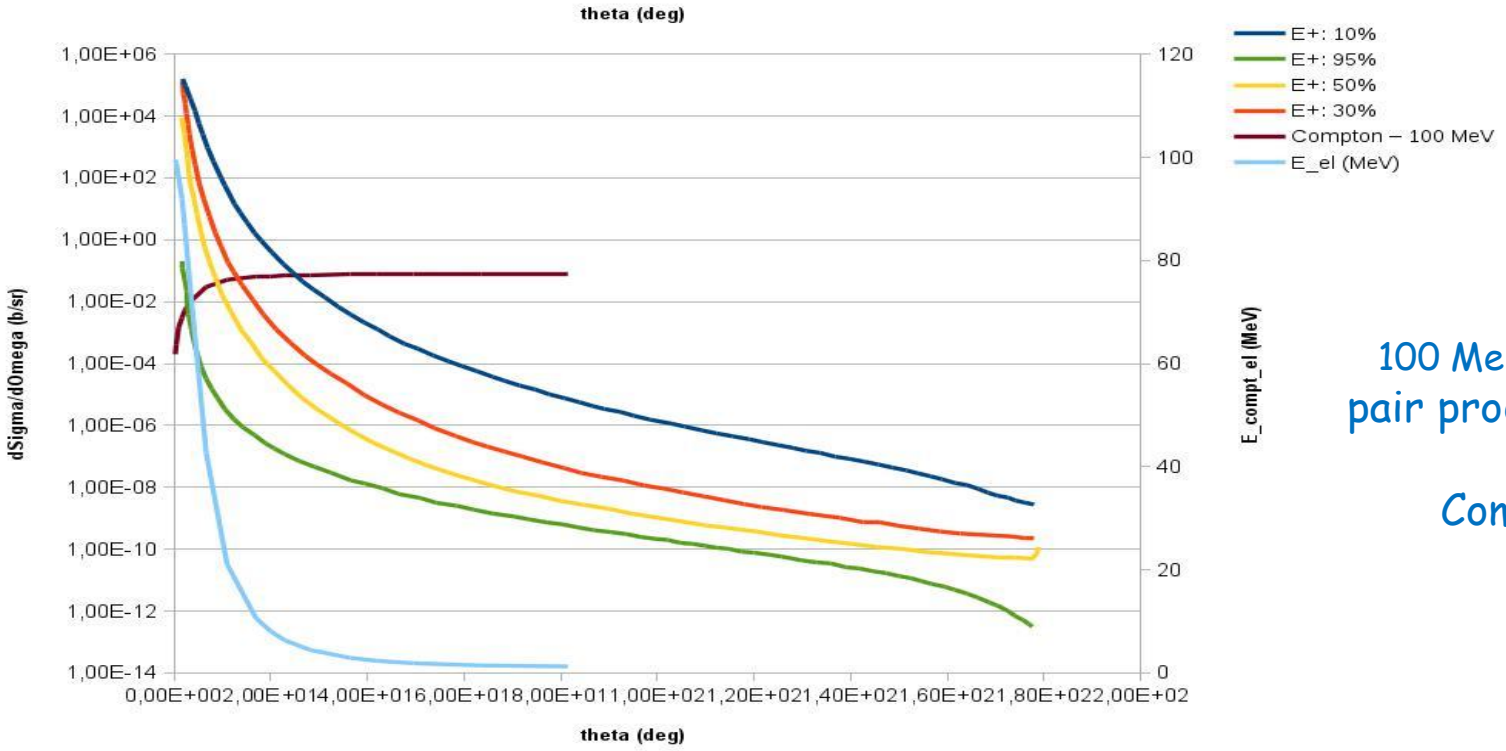

100 MeV γ on nitrogen
pair prod. & Compton CS
AND
$Compt_{el}$ energy

Production of short duration mono-energetic neutron pulses Experiment at Titan/LLNL (USA)

Spokesperson: J. Fuchs (LULI) et al.

Plastic scintillator (4x4x12 cm^3) couplet to PMT

32 channel switch capacitor digitizer

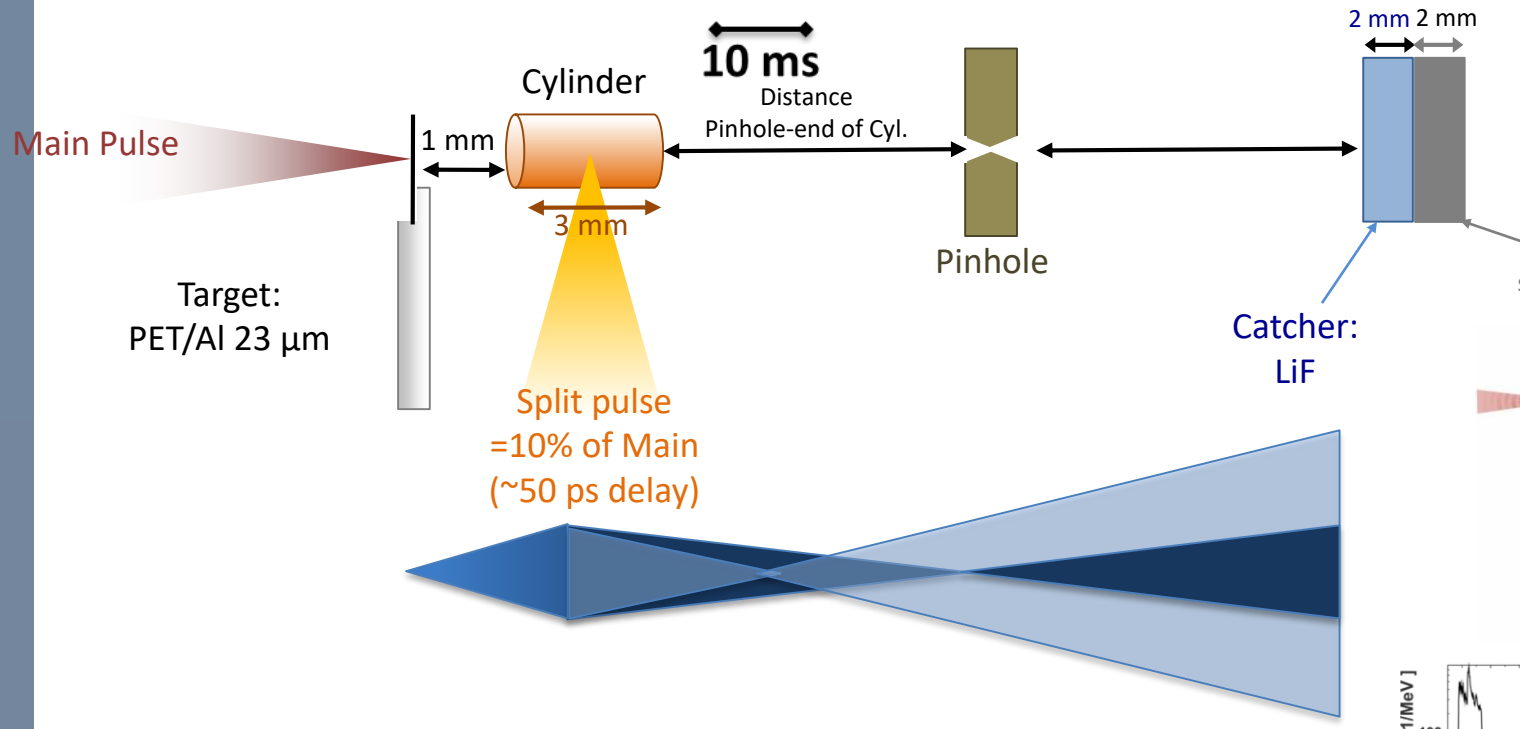

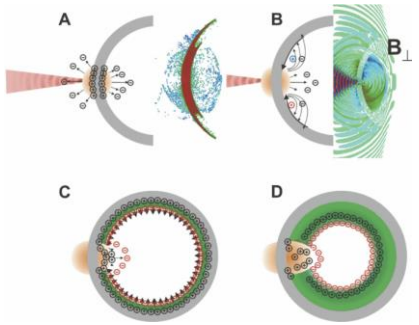

Longer focal length for more energetic protons

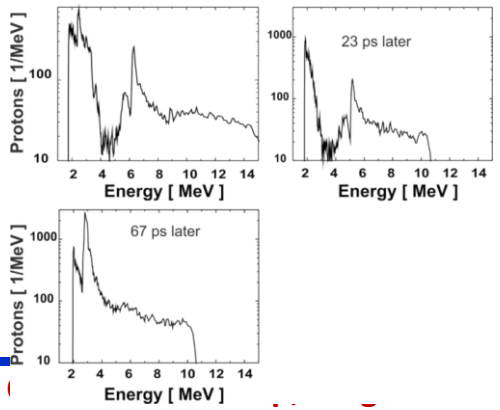

Detailed study of the method in:
T. Toncian at al., AIP Advances 1, 022142 (2011)

Fast neutron detection with plastic scintillator

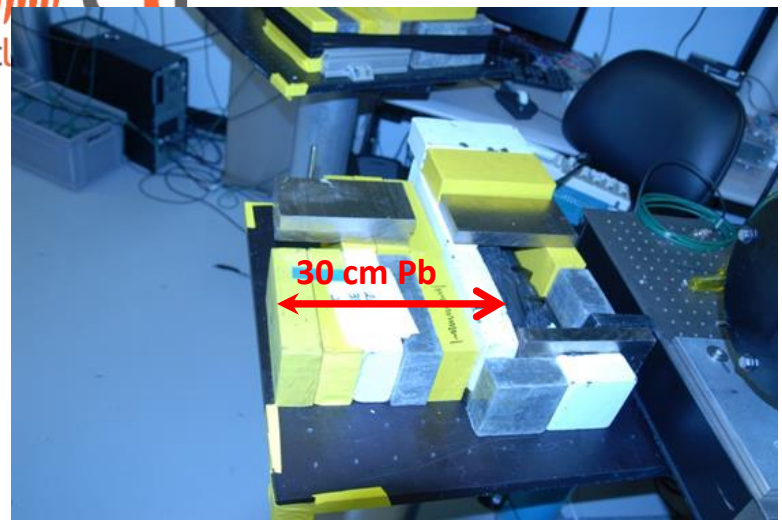

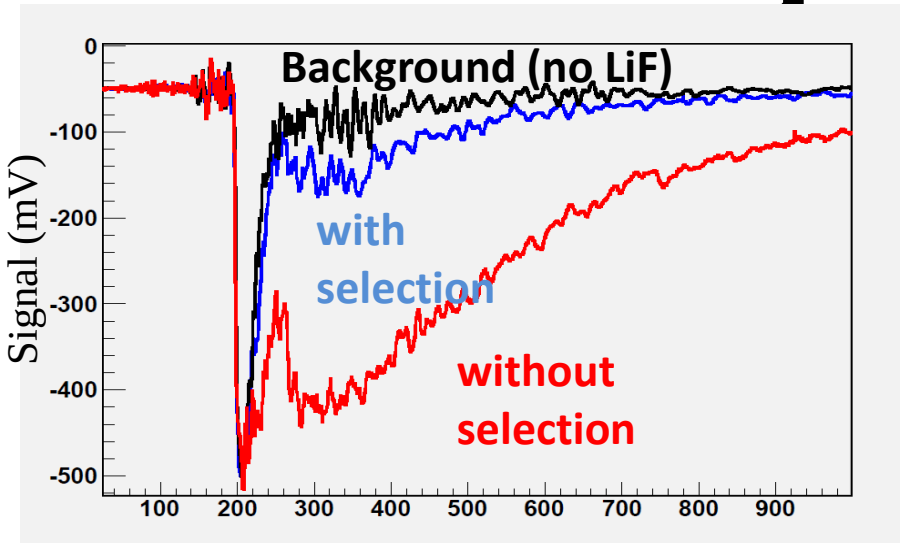

On-going Geant4 simulation to extract neutron spectrum from the measured waveform

- **High granularity detector system proposed at ELI-NP:**
  small volume and ~ 1000 segments => Single neutron event in detector per shot
- **Try SiPM (silicon photomultipliers) instead of dynode PMT**
  - **PA shielding against EMP**
  - **test gating (polarization needed is ~ tens V)**

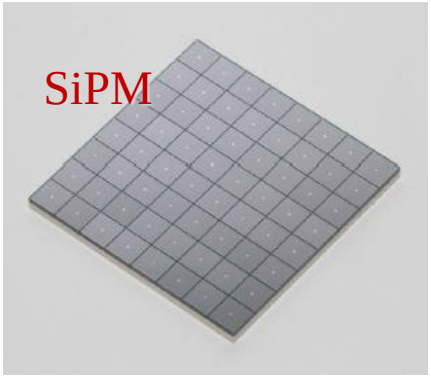

HAMAMATSU

- compact
- high photo-detection efficiency
- high gain
- single photon sensibility
- excellent timing performance
- low operative voltage
- insensitivity to large electric and magnetic fields

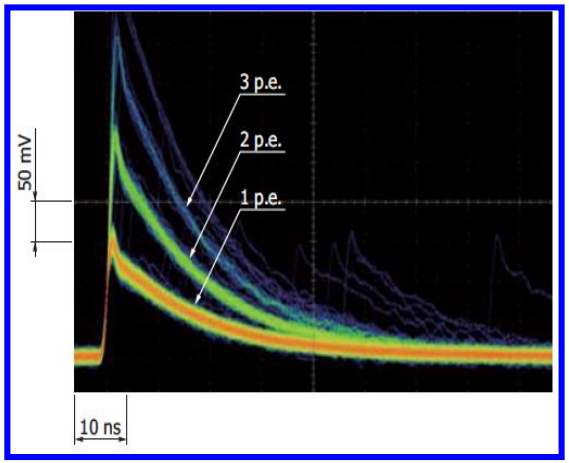

TNT acquisition

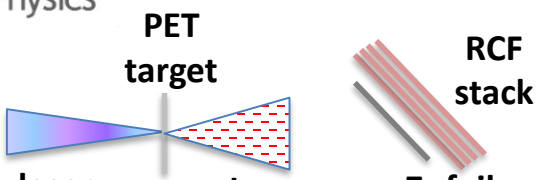

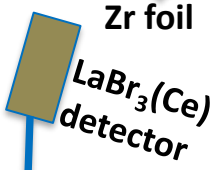

Fast Amplifier

Digitizer with PSA
14 bits - 100 MS/s

Oscilloscope
(Traces @ 250 MS/s)

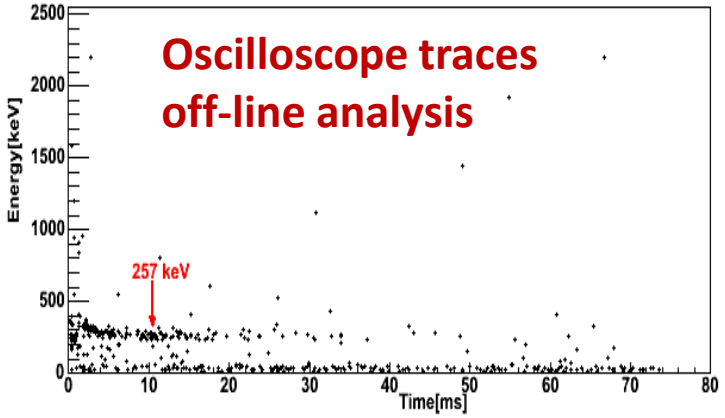

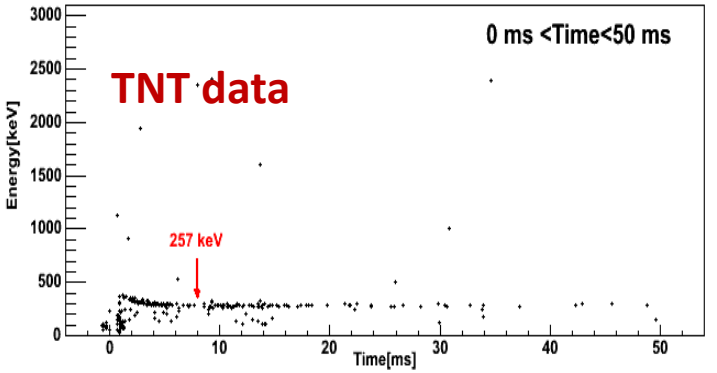

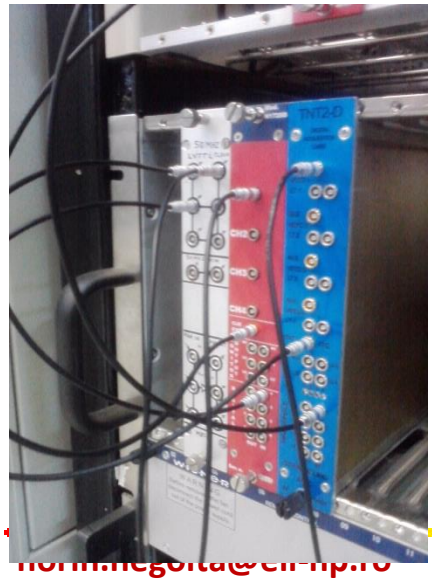

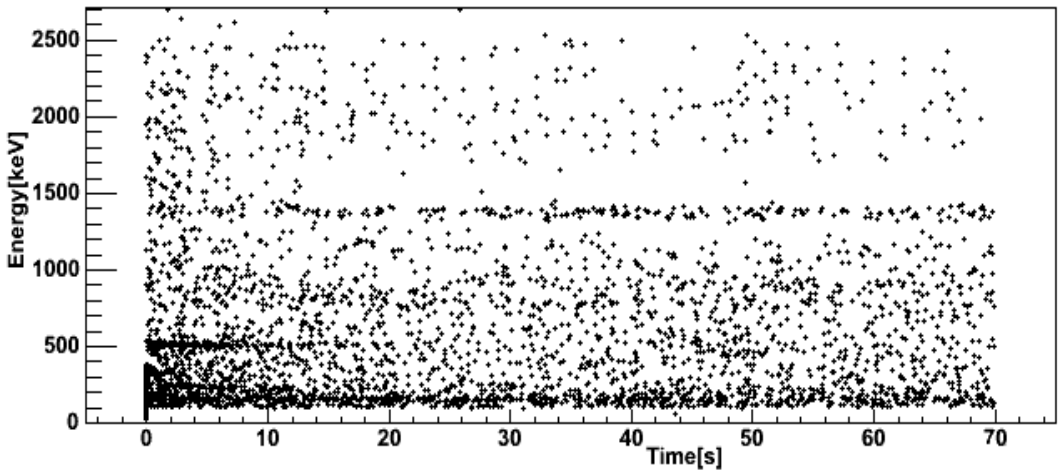

"*In Situ*" Gamma Spectroscopy. Yield calculation.

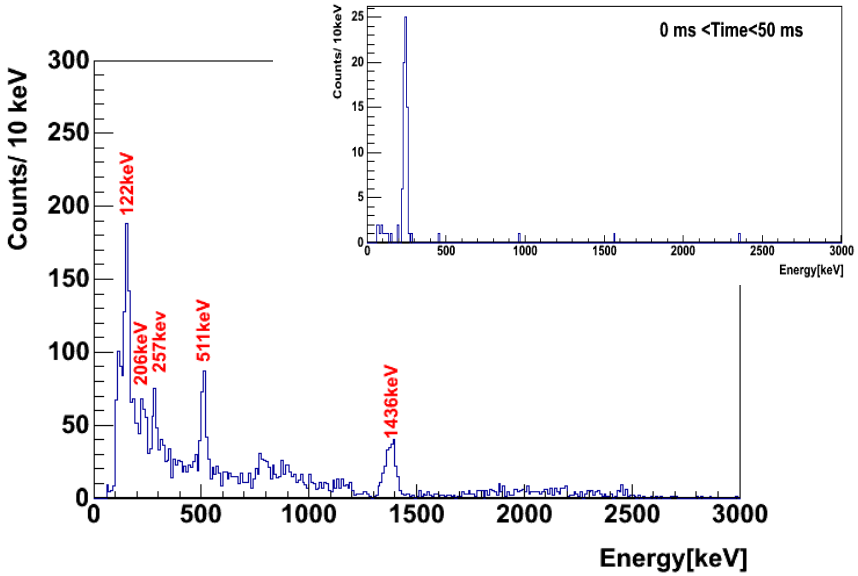

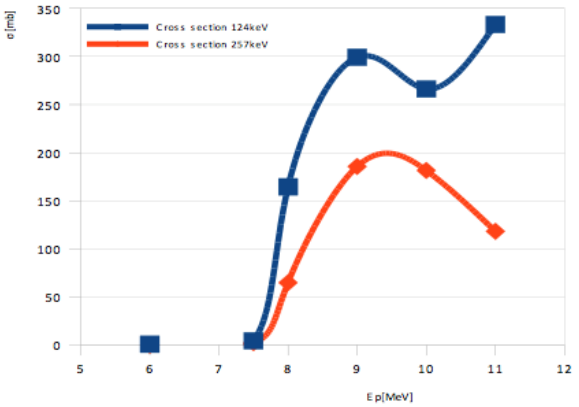

Calculated cross sections for isomer population to be convoluted with measured proton spectrum to get calculated yield.

Shot	E_g (keV)	Time gate (ms)	Exp. Area	Eff.	Exp. $Yield_g$	Calc. $Yield_g$	Exp/Calc Ratio
Tir80	122	5 – 1e5	254	1.5e-3	1.7e5	9.3e4	1,19
Tir81	122	5 – 1e5	136	1.5e-3	9.2e4	4.9e4	1.05
Tir115	122	5 – 1e5	79	1.5e-3	5.4e4	3.6e4	1.02
Tir80	257	5 – 100	121	1.2e-3	1.8e5	7.1e4	1.40
Tir81	257	5 – 100	67	1.2e-3	9.7e4	3.7e4	0.83
Tir115	257	5 – 100	31	1.2e-3	4.5e4	2.7e4	0.99

"*In Situ*" Gamma Spectroscopy can used as on line ion diagnostics.

Ion diagnostics: "*In Situ*" Gamma Spectroscopy

Estimations of cross section for production of short lived nuclear states using TALYS code and fusion-evaporation cross section using PACE-IV code.

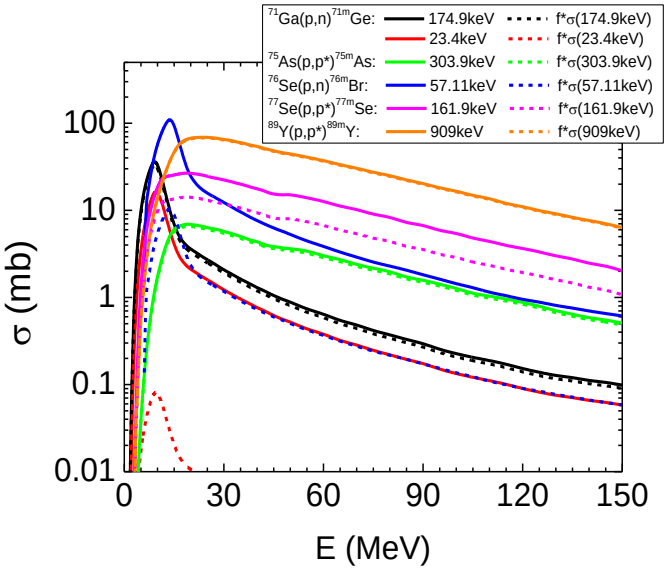

Calculated cross section for production isomeric states in proton induced reaction.

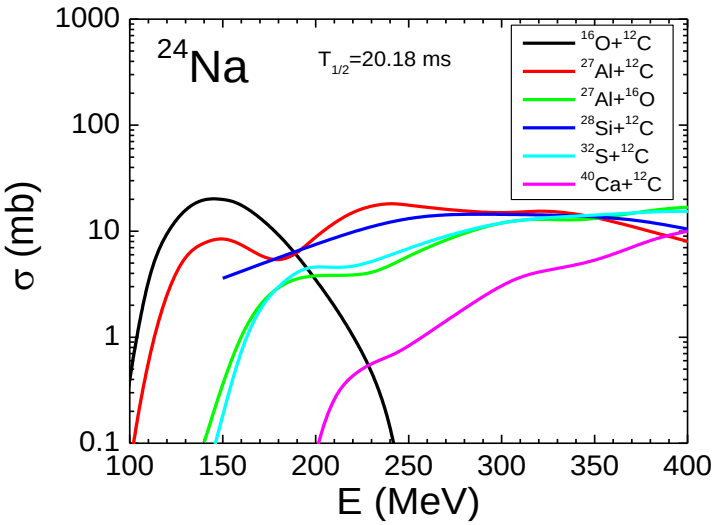

Calculated cross section for ^{24}Na in reactions induced by ^{12}C and ^{16}O projectiles.

Ion diagnostics: "*In Situ*" Gamma Spectroscopy
Nuclear states of interest and nuclear reactions tracked for estimation of production cross section of short lived states.

Isomer	E_{lev} (keV)	$T_{1/2}$	Jπ	Reaction
^{24}Na	472.2074	20.19ms	1+	^{12}C+^{16}O, ^{27}Al+^{12}C, ^{27}Al+^{16}O, ^{28}Si+^{12}C, ^{32}S+^{12}C, ^{40}Ca+^{12}C
^{24}Al	425.8	130ms	1+	^{12}C+^{16}O, ^{27}Al+^{12}C, ^{27}Al+^{16}O, ^{28}Si+^{12}C
^{26}Al	228.305	6.3452s	0+	^{12}C+^{16}O, ^{27}Al+^{12}C, ^{27}Al+^{16}O, ^{28}Si+^{12}C, ^{28}Si+^{16}O, ^{32}S+^{12}C, ^{32}S+^{16}C, ^{40}Ca+^{12}C
^{38}Cl	671.365	715ms	5-	^{27}Al+^{16}O, ^{28}Si+^{16}O, ^{32}S+^{12}C, ^{32}S+^{16}C, ^{40}Ca+^{12}C, ^{40}Ca+^{16}O
^{38}K	130.4	924ms	0+	^{27}Al+^{12}C, ^{27}Al+^{16}O, ^{28}Si+^{12}C, ^{28}Si+^{16}O, ^{32}S+^{12}C, ^{32}S+^{16}C, ^{40}Ca+^{12}C, ^{40}Ca+^{16}O
^{40}Sc	0	182.3ms	4-	^{28}Si+^{16}O, ^{32}S+^{12}C, ^{32}S+^{16}C, ^{40}Ca+^{12}C
^{44}V	0	111ms	(2)+	^{32}S+^{16}C, ^{40}Ca+^{12}C, ^{40}Ca+^{16}O
^{54}Co	0.0	193.28ms	0+	^{40}Ca+^{16}O
^{68}Se	0	35.5s	0+	^{66}Zn+^{12}C, ^{66}Zn+^{16}O, ^{68}Zn+^{16}O
^{73}Ge	66.726	0.499s	½-	^{66}Zn+^{12}C, ^{66}Zn+^{16}O, ^{68}Zn+^{12}C, ^{68}Zn+^{16}O, ^{69}Ni+^{12}C
^{75}As	303.9343	17.62ms	9/2+	^{66}Zn+^{12}C, ^{66}Zn+^{16}O, ^{68}Zn+^{12}C, ^{68}Zn+^{16}O, ^{69}Ni+^{12}C
^{76}Br	102.58	1.31s	(4)+	^{66}Zn+^{12}C, ^{66}Zn+^{16}O, ^{68}Zn+^{12}C, ^{68}Zn+^{16}O

Gamma induced activation

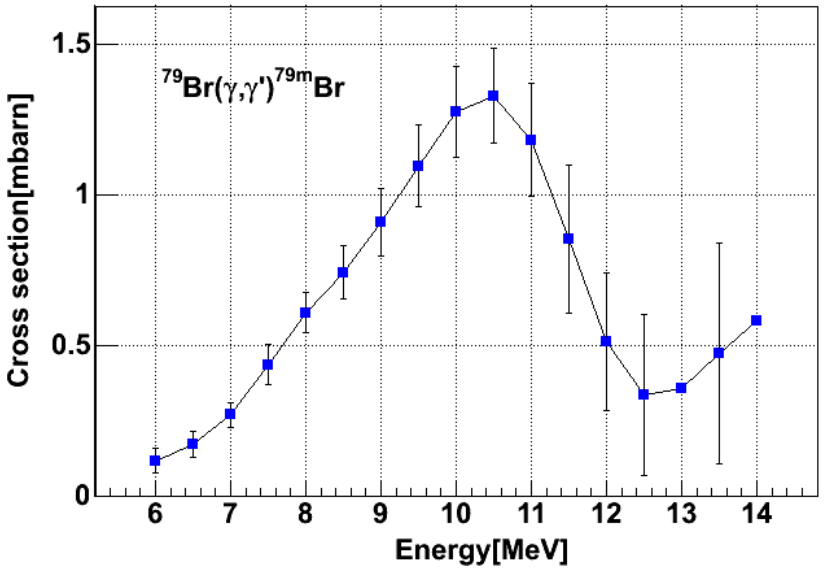

Inelastic excitation of 79Br
(207.6 keV, $T_{1/2}$=5.1 s)

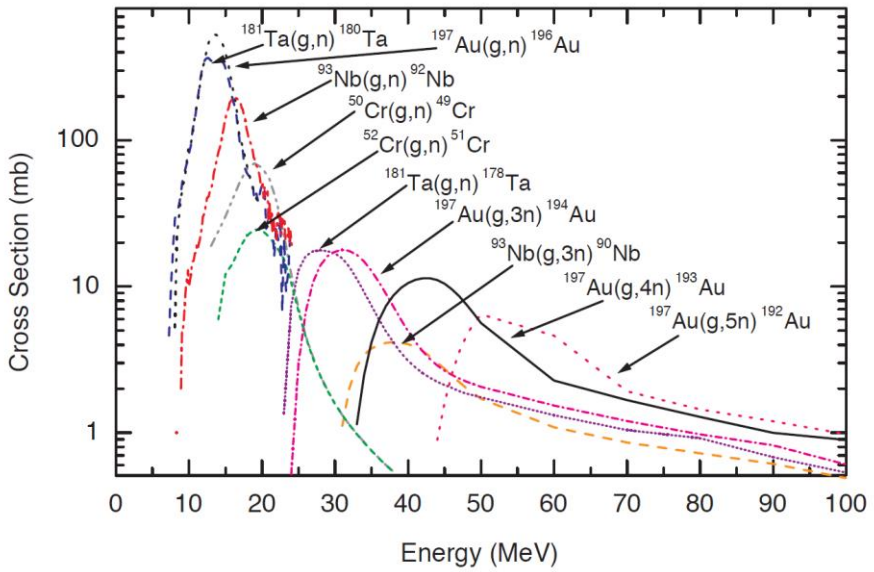

M.Roth, JINST 6 (2011) R09001

"In Situ" Gamma Spectroscopy can used as on line gamma spectrum diagnostics.

Gamma induced ms isomer population

IFIN-HH

Reaction	Abv	Abund (%)	E_{lev} (keV)	E_γ (keV)	$J\pi^{isom}$	$T_{1/2}$	$T_{1/2}^{isom}$	$E_{threshold}$ (MeV)
$^{25}_{12}Mg+\gamma \rightarrow {}^{24}_{11}Na+p$	(γ,p)	10	472.2	472.2	1+	14.997 h	20.18 ms	12.54
$^{40}_{19}K+\gamma \rightarrow {}^{38}_{17}Cl+2p$	(γ,2p)	0.012	671.4	671.4	5–	37.24 m	715 ms	21
$^{40}_{19}K+\gamma \rightarrow {}^{38}_{19}K+2n$	(γ, 2n)		130.4	no γ	0+	7.636 m	924 ms	21
$^{45}_{21}Sc+\gamma \rightarrow {}^{45}_{21}Sc+\gamma$	(γ, γ)	100.0	12.4	12.4	3/2+	STABLE	318 ms	0.0124
$^{72}_{32}Ge+\gamma \rightarrow {}^{71}_{32}Ge+n$	(γ, n)	27.40	198.4	23.438	9/2+	11.43 d	20.41 ms	10.94
$^{73}_{32}Ge+\gamma \rightarrow {}^{73}_{32}Ge+\gamma$	(γ, γ)		66.7	53.44	1/2–	STABLE	499 ms	0.067
$^{73}_{32}Ge+\gamma \rightarrow {}^{72}_{31}Ga+p$	(γ, p)	7.80	119.65	103.14	(0+)	14.10 h	39.68ms	10.12
$^{73}_{32}Ge+\gamma \rightarrow {}^{71}_{32}Ge+2n$	(γ, 2n)		198.4	23.438	9/2+	11.43 d	20.41ms	17.73
$^{74}_{32}Ge+\gamma \rightarrow {}^{73}_{32}Ge+n$	(γ, n)		66.7	53.44	1/2–	STABLE	499 ms	10.3
$^{74}_{32}Ge+\gamma \rightarrow {}^{72}_{31}Ga+d$	(γ, d)	36.50	119.65	103.14	(0+)	14.10 h	39.68 ms	18.09
$^{74}_{32}Ge+\gamma \rightarrow {}^{71}_{32}Ge+3n$	(γ, 3n)		198.4	23.438	9/2+	11.43 d	20.41 ms	27.9
$^{75}_{33}As+\gamma \rightarrow {}^{75}_{33}As+\gamma$	(γ, γ)		303.92	303.92	9/2+	STABLE	17.62 ms	26.35
$^{75}_{33}As+\gamma \rightarrow {}^{73}_{32}Ge+d$	(γ, d)	100.0	66.7	53.44	1/2–	STABLE	499 ms	14.93
$^{75}_{33}As+\gamma \rightarrow {}^{72}_{31}Ga+t$	(γ, t)		119.65	103.14	(0+)	14.10 h	39.68ms	19.5
$^{75}_{33}As+\gamma \rightarrow {}^{71}_{32}Ge+\alpha$	(γ, α)		198.4	23.438	9/2+	11.43 d	20.41 ms	26.35
$^{89}_{39}Y+\gamma \rightarrow {}^{88}_{39}Y+n$	(γ, n)	100.0	392.86 674.55	392.86 442.62	1+ 8+	106.6 d	0.301 ms 13.98 ms	lev2→11.87 lev3→12.16
$^{90}_{40}Zr+\gamma \rightarrow {}^{90}_{40}Zr+\gamma$	(γ, γ)	51.45	2319	2318.9	5–	STABLE	809.2 ms	2.32
$^{90}_{40}Zr+\gamma \rightarrow {}^{88}_{39}Y+d$	(γ, d)		392.86 674.55	392.86 442.62	1+ 8+	106.6 d	0.301 ms 13.98 ms	lev2→18.00 lev3→18.28
$^{91}_{40}Zr+\gamma \rightarrow {}^{90}_{40}Zr+n$	(γ, n)	11.27	2319	2318.9	5–	STABLE	809.2 ms	9.51
$^{91}_{40}Zr+\gamma \rightarrow {}^{88}_{39}Y+t$	(γ, t)		392.86 674.55	392.86 442.62	1+ 8+	106.6 d	0.301 ms 13.98 ms	lev2→18.94 lev3→19.22
$^{92}_{40}Zr+\gamma \rightarrow {}^{90}_{40}Zr+2n$	(γ, 2n)	17.17	2319	2318.9	5–	STABLE	809.2 ms	18.14
$^{92}_{41}Nb+\gamma \rightarrow {}^{90}_{40}Zr+d$	(γ, d)		2319	2318.9	5–	STABLE	809.2 ms	13.13
$^{92}_{41}Nb+\gamma \rightarrow {}^{90}_{41}Nb+2n$	(γ, 2n)		382.01	257.34	1+	14.60 h	6.19 ms	20.32
$^{92}_{41}Nb+\gamma \rightarrow {}^{88}_{39}Y+\alpha$	(γ, α)		392.86 674.55	392.86 442.62	1+ 8+	106.6d	0.301 ms 13.98 ms	lev2→4.97 lev3→5.25
$^{92}_{42}Mo+\gamma \rightarrow {}^{89}_{42}Mo+3n$	(γ, 3n)	14.84	387.5	268.6	(1/2–)	2.11 m	190 ms	36.4
$^{92}_{42}Mo+\gamma \rightarrow {}^{90}_{41}Nb+d$	(γ, d)		382.01	257.34	1+	14.60 h	6.19 ms	17.66
$^{92}_{42}Mo+\gamma \rightarrow {}^{90}_{40}Zr+2p$	(γ, 2p)		2319	2318.9	5–	STABLE	809.2 ms	14.93
$^{104}_{44}Ru+\gamma \rightarrow {}^{103}_{44}Ru+n$	(γ, n)	18.70	238.2	24.6	11/2–	39.25 d	1.69 ms	9.14
$^{104}_{44}Ru+\gamma \rightarrow {}^{101}_{43}Tc+t$	(γ, t)		207.5	191.92	1/2–	14.22 m	0.64 ms	16.9
$^{105}_{46}Pd+\gamma \rightarrow {}^{103}_{44}Ru+2p$	(γ, 2p)	22.33	238.2	24.6	11/2–	39.247d	1.69 ms	15.97

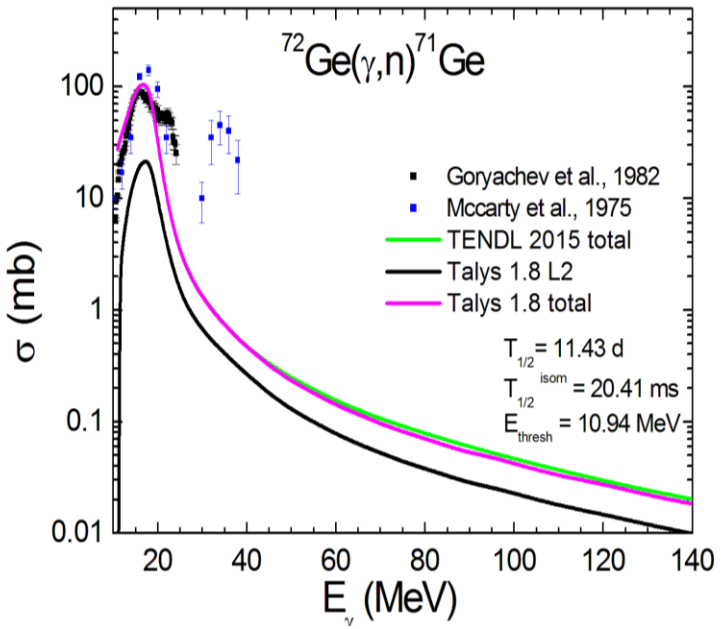

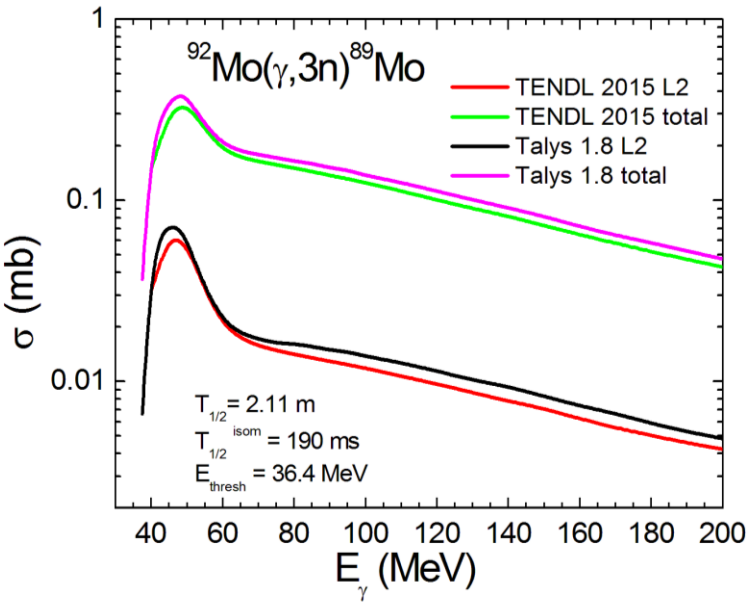

X-ray Backlighter for High Density Plasma Characterisation

Proposal of D. Stutman et al.

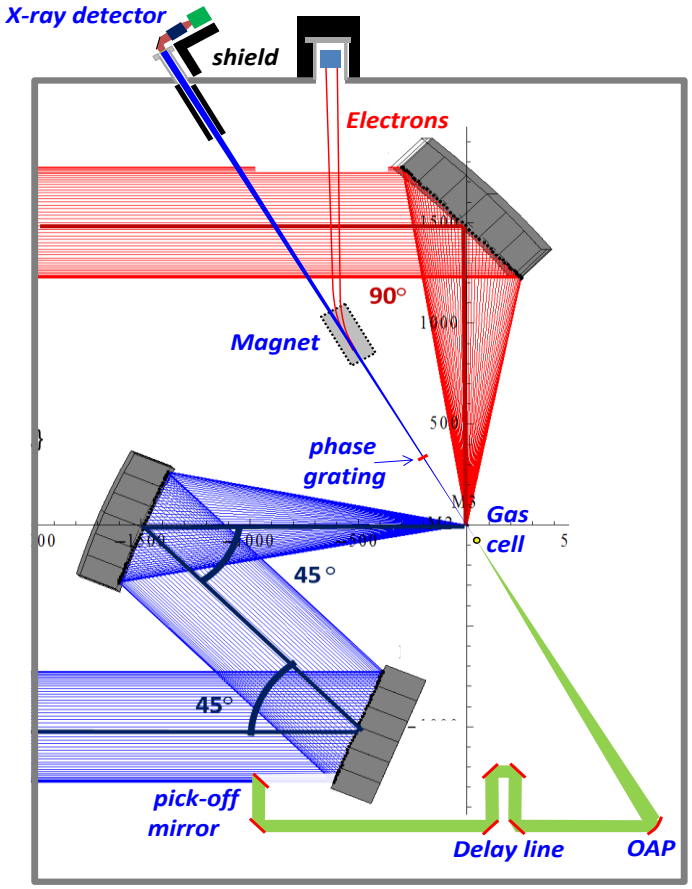

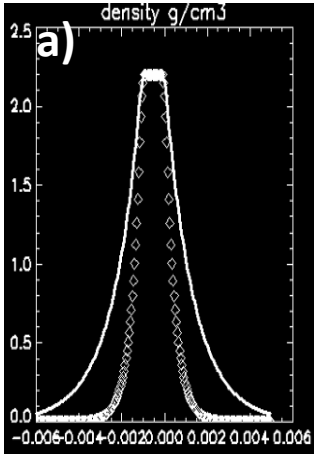

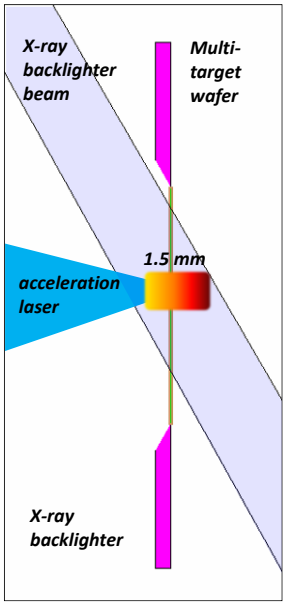

Zoom around target position

Two target density profiles assumed in the simulation, and calculated X-ray intensity profiles.

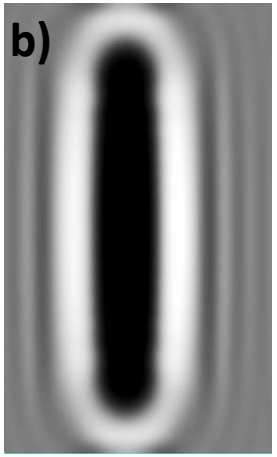

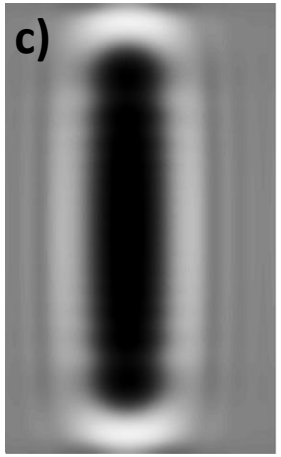

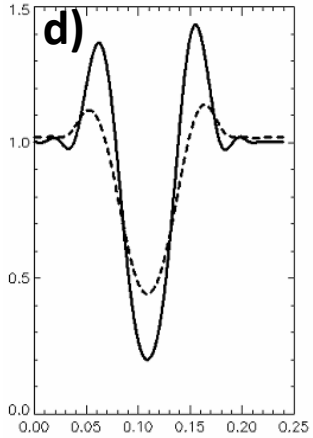

Using betatron emission occuring during LWFA electron acceleration in gas as probe beam for high density plasma.

Beam-dump

Source Label	Particle	Mean Energy (GeV)	Particles / Pulse	Freq. (Hz)	Div[2]	Spectrum	FWHM (GeV)
A	Proton	0.5	1.40E+12	1/60	40^0	Rectangular	0.05
	Electron	1.5	8.00E+10			Gaussian	0.15
B	Proton	0.04	1.00E+14	1/60	40^0	Boltzmann[1]	n/a

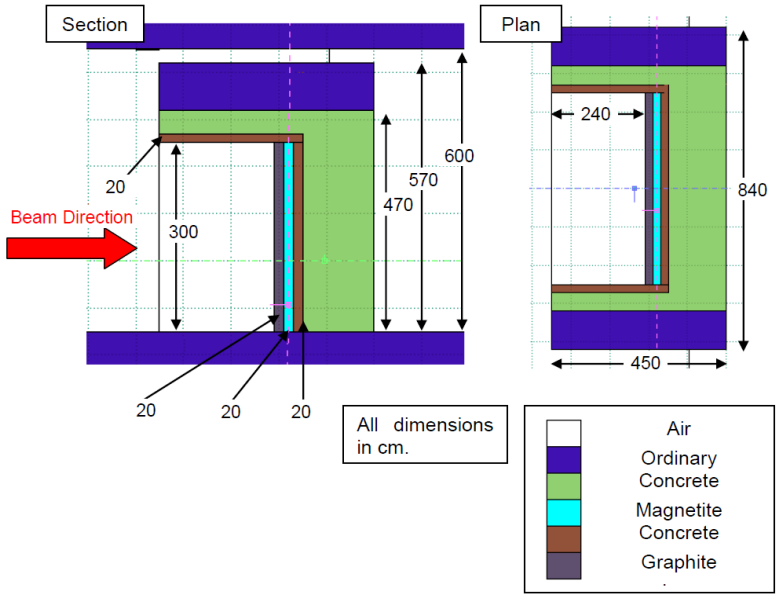

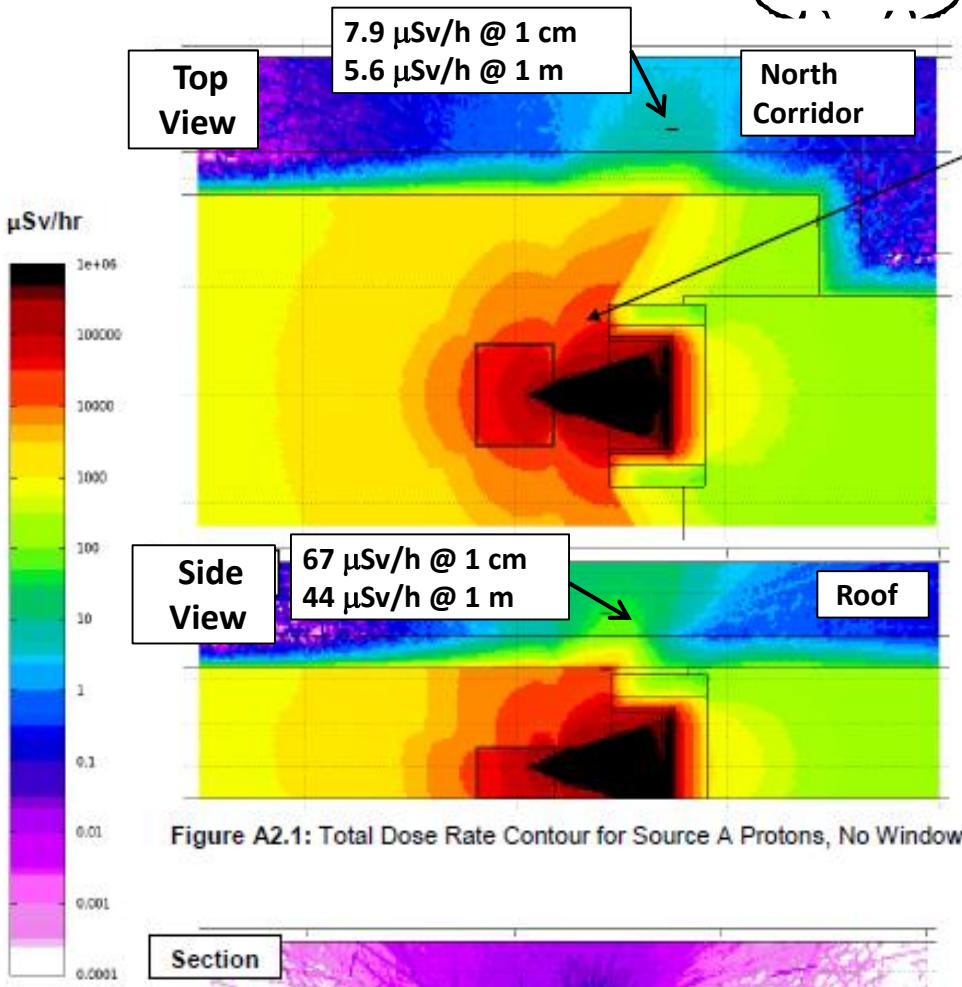

Figure A2.1: Total Dose Rate Contour for Source A Protons, No Window

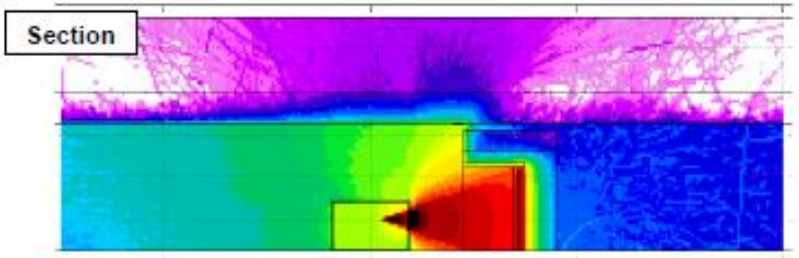

Figure A2.2: Total Dose Rate Contour from Source A Electrons, No Window (Section Only)

- Total mass of beam-dump: 525 tons
- Additional shielding under evaluations:
  - to reduce *prompt doses* on corridor
  - to access the target if *activation* too high

EUROPEAN UNION

GOVERNMENT OF ROMANIA

Structural Instruments 2007-2013

Sectoral Operational Programme "Increase of Economic Competitiveness"

"Investments for Your Future!"

IFIN-HH

Extreme Light Infrastructure - Nuclear Physics (ELI-NP) - Phase II

eli Nuclear Physics

www.eli-np.ro

Project co-financed by the European Regional Development Fund

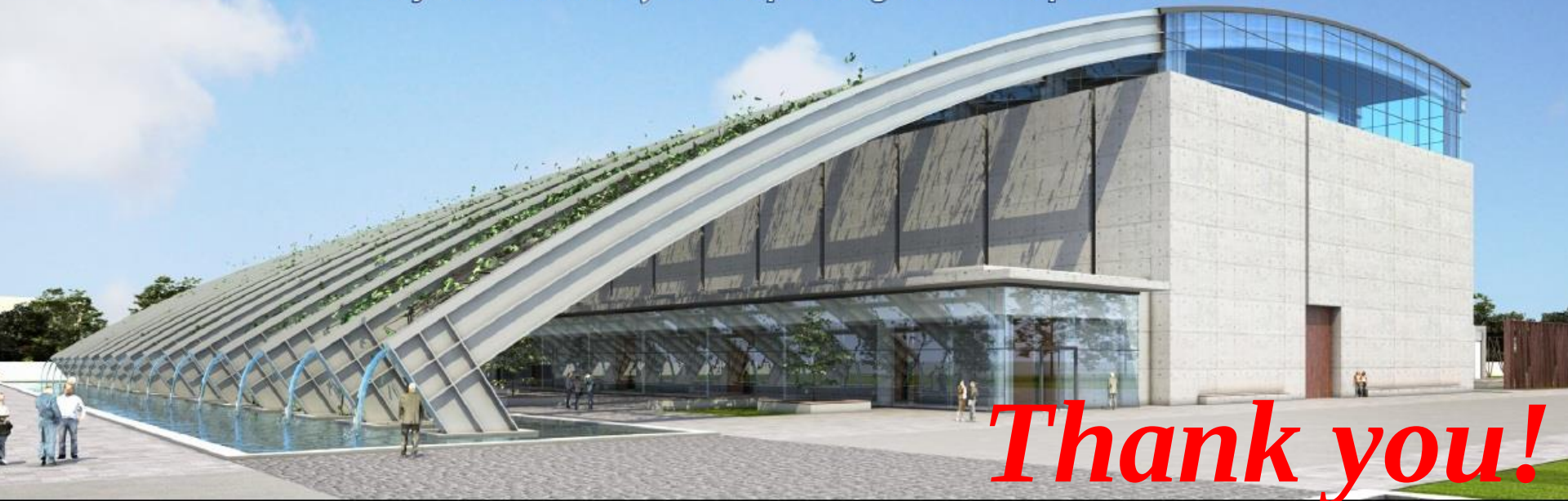

Thank you!